



HAL
open science

The SLX4 Complex Is a SUMO E3 Ligase that Impacts on Replication Stress Outcome and Genome Stability

Jean-Hugues Guervilly, Arato Takedachi, Valeria L Naim, Sarah Scaglione, Charly Chawhan, Yoann L Lovera, Emmanuelle L Despras, Isao Kuraoka, Patricia L Kannouche, Filippo L Rosselli, et al.

► To cite this version:

Jean-Hugues Guervilly, Arato Takedachi, Valeria L Naim, Sarah Scaglione, Charly Chawhan, et al.. The SLX4 Complex Is a SUMO E3 Ligase that Impacts on Replication Stress Outcome and Genome Stability. *Molecular Cell*, 2015, 57 (1), pp.123-137. 10.1016/j.molcel.2014.11.014 . hal-01429041

HAL Id: hal-01429041

<https://amu.hal.science/hal-01429041>

Submitted on 6 Jan 2017

HAL is a multi-disciplinary open access archive for the deposit and dissemination of scientific research documents, whether they are published or not. The documents may come from teaching and research institutions in France or abroad, or from public or private research centers.

L'archive ouverte pluridisciplinaire **HAL**, est destinée au dépôt et à la diffusion de documents scientifiques de niveau recherche, publiés ou non, émanant des établissements d'enseignement et de recherche français ou étrangers, des laboratoires publics ou privés.

TITLE: The SLX4 Complex Is a SUMO E3 Ligase that Impacts on Replication Stress Outcome and Genome Stability

AUTHORS:

Jean-Hugues Guervilly^{1,2,6}, Arato Takedachi^{1,2,6}, Valeria Naim³, Sarah Scaglione^{1,2}, Charly Chawhan⁴, Yoann Lovera^{1,2}, Emmanuelle Despras³, Isao Kuraoka⁵, Patricia Kannouche³, Filippo Rosselli³, Pierre-Henri L. Gaillard^{1,2}.

¹Centre National de la Recherche Scientifique, Unité Mixte de Recherche 7258, Inserm-Unité 1068, Centre de Recherche en Cancérologie de Marseille, Institut Paoli-Calmettes, France

²Aix-Marseille Université, F-13284, Marseille, France

³Université Paris-Sud, UMR 8200 CNRS, Equipe Labélisée La Ligue Contre le Cancer, Institut Gustave Roussy, 114 rue Edouard Vaillant, 94805, Villejuif Cedex, France.

⁴Genome Damage and Stability Centre, University of Sussex, Brighton, BN1 9RQ, UK

⁵Division of Chemistry, Graduate School of Engineering Science, Osaka University

⁶These authors contributed equally to this work

RUNNING TITLE: SUMO-related functions of SLX4

CONTACT:

Dr. Pierre-Henri Gaillard (pierre-henri.gaillard@inserm.fr)

Dr. Jean-Hugues Guervilly (jean-hugues.guervilly@inserm.fr)

SUMMARY:

The SLX4 Fanconi anemia protein is a tumor suppressor that may act as a key regulator that engages the cell into specific genome maintenance pathways. Here, we show that the SLX4 complex is a SUMO E3 ligase that SUMOylates SLX4 itself and the XPF subunit of the DNA repair/recombination XPF-ERCC1 endonuclease. This SLX4-dependent activity is mediated by a remarkably specific interaction between SLX4 and the SUMO-charged E2 conjugating enzyme UBC9 and not only relies on newly identified SUMO interacting motifs (SIMs) in SLX4 but also on its BTB domain. In contrast to its ubiquitin-binding UBZ4 motifs, SLX4 SIMs are dispensable for its DNA interstrand crosslink repair functions. Instead, while detrimental in response to global replication stress, the SUMO E3 ligase activity of the SLX4 complex is critical to prevent mitotic catastrophe following common fragile sites expression.

INTRODUCTION:

DNA damage triggers a complex network of signal transduction pathways that coordinate progression of the cell cycle with DNA replication, repair and recombination. Accumulating evidence suggests that the SLX4 protein may fulfill key functions in these coordination mechanisms. In both *Saccharomyces cerevisiae* (*S. cerevisiae*) and *Schizosaccharomyces pombe* Slx4 is essential for viability in absence of the BLM-related helicases Sgs1 and Rqh1, respectively, and controls the stability of the rDNA locus by binding and stimulating the Slx1 structure-specific endonuclease (Coulon et al., 2004; Kaliraman and Brill, 2002). In *S. cerevisiae*, it also participates in repair of DNA double-strand breaks (DSBs) by binding to the Rad1-Rad10 structure-specific endonuclease and stimulating the removal of 3'

single-strand overhangs during single-strand annealing (Toh et al., 2010) while it acts with the Rtt107 scaffold in recovery from replisome stalling (Flott et al., 2007).

Human SLX4 not only interacts with SLX1 and XPF^{Rad1}-ERCC1^{Rad10} as in yeast, but also with the MUS81-EME1 Holliday junction (HJ) resolvase (Fekairi et al., 2009; Munoz et al., 2009; Svendsen et al., 2009), the MSH2-MSH3 mismatch repair complex, the telomeric TRF2 protein, as well as with the PLK1 cell-cycle control kinase (Fekairi et al., 2009; Svendsen et al., 2009). Interestingly, metazoan SLX4 has acquired a large N-terminal extension with several additional protein-protein interaction domains including ubiquitin binding UBZ4 zinc fingers, a so-called MLR motif involved in direct interaction with XPF^{Rad1} and a BTB domain possibly involved in protein-protein interaction and oligomerization (Andersen et al., 2009; Fekairi et al., 2009; Munoz et al., 2009; Svendsen et al., 2009).

Along with XPF-ERCC1, SLX4 is essential for DNA interstrand crosslink repair (ICL) (Douwel et al., 2014; Fekairi et al., 2009; Hodskinson et al., 2014; Kim et al., 2013; Munoz et al., 2009; Svendsen and Harper, 2010). Confirming initial suggestions that SLX4 may act in the Fanconi anemia (FA) ICL repair pathway (Fekairi et al., 2009), mutations in SLX4 have been found as causative of FA, a rare genetic disease associated with bone marrow failure, cancer predisposition, chromosome instability and hypersensitivity to DNA crosslinking agents (Kim et al., 2011; Stoepker et al., 2011). Moreover, *Slx4*^{-/-} mice phenocopy FA (Crossan et al., 2011) and develop multiple cancers underlining the fundamental importance of SLX4 as a tumor suppressor (Hodskinson et al., 2014).

SLX4 is also critical along with SLX1 and MUS81-EME1 for chromosome segregation and cell viability in absence of the Bloom syndrome (BS) helicase BLM, which acts to

“dissolve” double Holliday junctions (HJ) formed by homologous recombination and prevent crossing over (Ashton et al., 2011; Wechsler et al., 2011; Wu and Hickson, 2003). BS is associated with remarkable chromosomal instability and cancer predisposition. In absence of BLM, HJ removal relies exclusively on GEN1 or SLX4-SLX1 and MUS81-EME1 HJ resolvases and is associated with high frequency of crossing over and an increased risk of loss of heterozygosity (Wechsler et al., 2011), (Castor et al., 2013; Wyatt et al., 2013). Combined loss of BLM, SLX4-SLX1 and MUS81-EME1 activities results in chromosome rearrangements, anaphase bridges, aberrant mitosis and cell death (Garner et al., 2013; Wyatt et al., 2013). Importantly, BLM and the FA pathway contribute to the stability of genomic loci that are challenging to replicate, such as common fragile sites (CFS) (Chan et al., 2009; Naim and Rosselli, 2009). SLX4 is also required for telomere stability through its direct interactions with TRF2, SLX1 and XPF-ERCC1 (Vannier et al., 2012; Wan et al., 2013; Wilson et al., 2013).

Although human SLX4 sits at the crossroads of genome maintenance and cell cycle control mechanisms, little is known as to how its various functions and those of its different partners are orchestrated. In this study, we identify SUMO-interacting motifs (SIMs) within SLX4 and demonstrate that they are required for the SUMOylation of SLX4 and XPF. *In vivo* and *in vitro* studies show that SLX4 specifically interacts with the charged SUMO E2 conjugating enzyme UBC9 and is a SUMO E3 ligase or an essential component of a multifactorial SUMO E3 ligase. This SUMO E3 ligase activity relies on the SIMs of SLX4 and, unexpectedly, its BTB domain. Importantly, we find that the SUMO E3 ligase activity of SLX4 is not required for its ICL repair functions. Instead, our data show that while this activity is detrimental in response to

global replication stress, it is critical to prevent mitotic catastrophe following CFS expression.

RESULTS

Human SLX4 is a SUMO-binding protein

We identified *in silico* three putative SUMO-interacting motifs (SIMs) in SLX4 conserved in metazoan (Figure 1A). To assess whether these are *bona fide* SIMs, we tested the ability of various recombinant SLX4 fragments produced in *E. coli* to bind SUMO3 chains. Immobilized His-MBP-tagged SLX4 fragments that contain two or three SIMs preferentially retained long poly-SUMO3 chains while no SUMO binding was observed with a fragment with no SIMs (Figure 1B). Importantly, mutating the aliphatic residues of the SIMs abrogated SUMO binding with a stronger impact of mutating SIM1 or SIM2 than mutating SIM3 (Figure 1C). *In vivo*, FLAG-SLX4 overproduced in human cells co-immunoprecipitated with both SUMO1- and SUMO2/3ylated proteins but not with free SUMO, while SIM mutated FLAG-SLX4 did not co-immunoprecipitate SUMOylated proteins (Figure 1D). Overall our data demonstrate that human SLX4 contains *bona fide* SIMs, preferentially binds poly-SUMO chains and interacts with SUMOylated proteins *in vivo*.

SLX4 SIMs mediate the SUMOylation of SLX4 and XPF *in vivo*

To undertake a functional characterization of the SIMs of SLX4, we generated stable, doxycycline (Dox)-inducible cell lines expressing YFP or FLAG-HA (F-HA)-tagged SLX4 using the Flp-In T-Rex system (hereafter designed as FIT₀ cells for the parental cell line with an empty Flp-In cassette). We first assessed whether SLX4 might be

SUMOylated, as reported for other SIM-containing proteins (Lin et al., 2006; Takahashi, 2004), and/or whether any of its partners are SUMOylated. The cell lines were transiently transfected with vectors driving over-production of His-SUMO and the E2 conjugating enzyme UBC9 to increase global SUMOylation. Only YFP-SLX4 and endogenous XPF were covalently modified by His-SUMO1 or His-SUMO3 *in vivo* and captured in denaturing His-pulldowns (Figure 2A; Figure S1A). Furthermore, SUMOylation was specific for XPF within the XPF-ERCC1 complex as no ERCC1 SUMOylation could be detected (data not shown). The migration pattern of SUMOylated SLX4 and XPF suggests that both proteins can undergo multiple mono-SUMOylation events and/or poly-SUMOylation (Figure 2A). SUMOylation of endogenous XPF was strongly stimulated in the cells that over-produce YFP-SLX4, suggesting that SLX4 up-regulates SUMOylation of XPF (Figure 2A). Consistent with this, SLX4 overexpression even promoted XPF SUMOylation in absence of SUMO over-production (Figure S1B) while SUMOylation of XPF was lost following depletion of SLX4 (Figure 2B). Most remarkably, the stimulatory effect of SLX4 was totally abolished in cells over-producing a SIM-mutated version of SLX4 (SLX4-SIM^{mut}) while it was unaffected in cells over-producing a UBZ-mutated protein (SLX4-UBZ^{mut}) (Figure 2C). SUMOylation of SLX4 itself was also SIM-dependent. Taken together, our data suggest that SLX4 controls SUMOylation of XPF and itself, and that this relies on its SIMs.

SUMOylation of XPF relies on optimal interaction with SLX4

To investigate whether SUMOylation of XPF relies on its association with SLX4 we generated SLX4 mutants defective in XPF-binding. One mutant was made by

mutating the MLR domain essential for the interaction between SLX4 and XPF (Fekairi et al., 2009; Svendsen et al., 2009) (Figure 2D). A direct interaction between XPF and the BTB domain of SLX4, a common protein-protein interaction and oligomerization domain (Perez-Torrado et al., 2006), was reported (Andersen et al., 2009). Therefore, we also generated an SLX4-BTB^{mut} mutant that was deficient for SLX4 dimerization (Figure S2A) and slightly impaired in XPF-binding (Figure 2D).

SLX4-MLR^{mut} was SUMOylated to the same extent as SLX4 but it was severely impaired in promoting XPF SUMOylation, indicating that XPF needs to bind to SLX4 to be SUMOylated *in vivo* (Figure 2E). Surprisingly, SLX4-BTB^{mut}, which was only mildly impacted in its ability to bind XPF (Figure 2D), was totally defective in promoting XPF SUMOylation (Figure 2E). Furthermore, SLX4-BTB^{mut} itself was not SUMOylated (Figure 2E). This was further confirmed with another BTB mutant of SLX4 (BTB^{mut2}) that was similarly defective in dimerization (Figure S2A) and in promoting SUMOylation of XPF and of itself (Figure S2B). However, in contrast to SLX4-SIM^{mut}, SLX4-BTB^{mut} bound SUMOylated proteins (Figure S2C) indicating that the stimulation of XPF SUMOylation by SLX4 and SUMOylation of SLX4 itself does not solely rely on its SUMO-binding properties.

SLX4 specifically interacts with charged UBC9

The strong up-regulation of XPF SUMOylation by over-production of SLX4 raised the possibility that SLX4 could be a SUMO E3 ligase or a component of a multi-subunit SUMO E3 ligase. To test this, we first assessed whether SLX4 directly interacts with the unique E2 SUMO conjugating enzyme UBC9, a characteristic of SUMO E3 ligases (Melchior, 2003; Seeler and Dejean, 2003). While we were able to detect an

SLX4-UBC9 interaction *in vivo* (Figure 3A), we failed to detect an interaction *in vitro* using recombinant UBC9 and SLX4 fragments (data not shown). A possible explanation was that SLX4 *in vivo* interacts only with SUMOylated UBC9 (UBC9_{SUMO}) and/or charged UBC9 engaged in a thioester linkage with SUMO (UBC9~SUMO), the active form of the E2 enzyme. To test this, we pre-incubated recombinant UBC9, E1 (SAE1-SAE2), SUMO2 and ATP before mixing with immobilized His-MBP-SLX4₆₈₄₋₁₂₀₆ (Figure 3B). A specific interaction was detected between SLX4₆₈₄₋₁₂₀₆ and a slow migrating form of UBC9 that appeared only when ATP was added during the pre-incubation (Figure 3C). To decipher whether this was charged UBC9~SUMO2 or SUMOylated UBC9_{SUMO2}, samples were reduced with DTT prior to gel electrophoresis to disrupt the thioester bond between UBC9 and SUMO in UBC9~SUMO without affecting UBC9_{SUMO2}. DTT converted the slow migrating form of UBC9 that bound to SLX4 to unmodified UBC9, indicating that SLX4 specifically interacts with UBC9~SUMO (Figure 3C). This specific interaction was almost totally abolished when the hydrophobic core of SLX4 SIMs were mutated (Figure 3C) but not when we deleted the BTB domain (Figure S3A). Both SLX4 SIM1 and SIM2 have clusters of acidic residues next to their hydrophobic core (Figure 3D). Such clusters are found in many SIMs and play a role in the SIM-SUMO associations (Kerscher, 2007). To assess the functional importance of these acidic residues, we generated “E/D” mutants by replacing aspartate and glutamate residues by alanine (Figure 3D). All three mutants had defects in SUMO chain binding (Figure S3B) and were unable to efficiently interact with UBC9~SUMO, suggesting that negative charges in SLX4 SIM1 and SIM2 may interact with the previously described basic patch of UBC9 spatially adjacent to its catalytic C93 residue (Mohideen et al., 2009). In support of

this, mutating the positively charged K65 or K74 residues of UBC9 severely reduced its interaction with SLX4₆₈₄₋₁₂₀₆ (Figure 3E). Importantly, the catalytic UBC9^{C93S} mutant which can be neither charged nor SUMOylated was unable to interact with SLX4 (Figure 3E). Together, our data suggest that the specific binding of SLX4 to charged UBC9~SUMO results from a bi-modal interaction that requires both SIM-SUMO recognition and electrostatic interactions between negatively charged residues in SIM1 and SIM2 and the basic patch of UBC9 (Figure 3F).

The SLX4 complex has SUMO E3 ligase activity

The specific interaction between SLX4 and charged UBC9 further suggested that SLX4 is an E3 SUMO ligase. However, we were unable to recapitulate efficient SLX4-mediated SUMOylation of XPF *in vitro* using recombinant SLX4 fragments (data not shown). Therefore, we adopted an *ex vivo/in vitro* strategy to monitor the SUMO E3 ligase activity of SLX4 immunoprecipitated from human cells and incubated with recombinant E1, UBC9 and SUMO2 (Figure 4A). As shown in Figure 4B, time dependent SUMOylation of both SLX4 and XPF could be recapitulated *in vitro* upon addition of ATP. In contrast, no SUMOylation was detected for MUS81, another co-purifying partner of SLX4 (Figure 4B). Importantly, none of the PIAS1, PIAS2, PIAS3, PIAS4, Pc2, MMS21, RANBP2 or KAP1 SUMO E3 ligases could be detected in SLX4 IPs (Figure S4). Furthermore, both SLX4-BTB^{mut} and SLX4-SIM^{mut} complexes were severely impaired in XPF and SLX4 SUMOylation (Figure 4C). This excludes a “non-specific” contribution of UBC9 that can bypass the need of an E3 ligase *in vitro* (Gareau and Lima, 2010). It also confirms that both the SIM and BTB domains of SLX4 are required for an efficient SLX4-dependent SUMO E3 ligase

activity towards XPF and itself. SUMOylation of XPF and SLX4 was severely reduced when using the UBC9 basic patch mutants K65A and K74A, underlining the functional importance of the SLX4/UBC9~SUMO interaction (Figure 4D). Interestingly, SUMO E3 ligase activity was decreased when the SLX4 immunoprecipitates were washed at 500 mM NaCl instead of 150 mM NaCl (Figure 4E). This suggested that robust SLX4-dependent SUMO E3 ligase activity relies on one or several salt-labile cofactors. Given that SLX4 participates in the DNA Damage Response, we wondered whether DNA itself may not stimulate the SLX4-dependent SUMO E3 ligase activity. Adding fragmented or undigested plasmid DNA to the SUMO ligase reaction restored XPF and SLX4 SUMOylation in 500 mM NaCl IPs to levels close to those achieved in 150 mM NaCl SLX4 IP (Figure 4F). Noteworthy, DNA was unable to stimulate SLX4-SIM^{mut} and SLX4-BTB^{mut} IPs at 150 mM NaCl (Figure 4G) and 500 mM NaCl (Data not shown), excluding a non-specific effect on poorly active SLX4 complexes. Finally, because SUMO ligase activity was detected only with the SLX4 complex from human cells and not with recombinant proteins we reasoned that PTMs may be required. Confirming this hypothesis, pre-incubating SLX4 IPs with lambda phosphatase reduced SUMOylation of XPF while heat-inactivated phosphatase had no effect (Figure 4H). Taken together, our data indicate that SLX4-dependent SUMO E3 ligase activity is strongly stimulated *in vitro* by DNA and that it partly relies on phosphorylation of SLX4 and/or one or several other components of the complex. These results along with the specific interaction of SLX4 with charged UBC9 and its role in controlling XPF SUMOylation *in vivo* show that SLX4 is a SUMO E3 ligase or an essential component of a multifactorial SUMO E3 ligase.

SUMO-related functions of SLX4 are not required for ICL repair but contribute to cellular toxicity induced by SLX4 overexpression

To gain further insight into the functional importance of the SUMO-related functions of SLX4 *in vivo*, we set up cell survival assays with our inducible cell-complementation system. Continuous overexpression of SLX4 at high doses of Dox was extremely cytotoxic (Figure 5A and 5B). Mutating the SIMs, but not the UBZs, partially alleviated this cytotoxicity while mutating the BTB domain further reduced toxicity (Figure 5B). These data suggest that the cytotoxicity induced by SLX4 overexpression is specifically associated with its SUMO-related functions. Cellular complementation assays were set-up by inducing mild expression of WT or mutant versions of YFP-SLX4 with a low dose of Dox and concomitant depletion of the endogenous protein (Figure S5). We first examined whether the SIM and BTB domains contribute to the well-established ICL repair function of SLX4. SLX4 was able to fully correct the MMC sensitivity induced by depletion of endogenous SLX4, while SLX4-UBZ^{mut} was totally defective in restoring resistance to MMC (Figure 5C), as expected from previous studies (Kim et al., 2011; 2013). SLX4 MLR^{mut} and SLX4 BTB^{mut} were also defective in restoring MMC resistance. These defects were expected because both SLX4 mutants are altered in their ability to bind XPF (Figure 2D) and because SLX4 and XPF-ERCC1 cooperate in ICL repair (Douwel et al., 2014; Hodskinson et al., 2014). In contrast, mild expression of SLX4 SIM^{mut} largely corrected the MMC sensitivity induced by depletion of endogenous SLX4 (Figure 5C). These results indicate that the SUMO E3 ligase activity of SLX4 is not critical in ICL

repair and suggest that instead it engages SUMOylated SLX4 and XPF in non-ICL repair pathways.

The SUMO E3 ligase activity of SLX4 mediates toxicity in response to global replication stress

Recent studies reported that SLX4 contributes to DSB formation in response to global replication stress (Couch et al., 2013; Fugger et al., 2013; Ragland et al., 2013). Our findings suggested that these effects might correlate with the SIM and BTB-dependent cytotoxicity induced by high over-expression levels of SLX4 (Figure 5B). Depletion of endogenous SLX4 in HeLa cells significantly enhanced cell survival in response to HU, while mild over-expression of YFP-SLX4 hyper-sensitized cells to HU and counteracted the positive impact of depleting endogenous SLX4 (Figure 6A and Figure S6A). Remarkably, this SLX4-mediated toxicity was abolished when the SIMs or the BTB domain of SLX4 were mutated (Figure 6A and Figure S6B) suggesting that SLX4-dependent SUMO E3 ligase activity is toxic in cells facing global replication fork stalling. Low doses of HU combined with ATR checkpoint kinase inhibition (ATRi) results in cell death associated with replication fork collapse, DSB induction and extensive ssDNA generation at the fork (Couch et al., 2013; Ragland et al., 2013). Depletion of SLX4 also attenuated the synthetic lethality of the double treatment HU+ATRi in the parental FIT₀ cells (Figure 6B). This rescue was counteracted by mild over-expression of SLX4 but not by SLX4-SIM^{mut} and SLX4-BTB^{mut}, indicating that the SLX4 SUMO E3 ligase activity also mediates toxicity in response to an acute replication stress (Figure 6B and S6B). We next wondered whether the SLX4-associated nucleases contribute to the SLX4-dependent

cytotoxicity induced by replication stress. Depletion of SLX1 or XPF-ERCC1, but not MUS81-EME1, enhanced cell survival following HU, albeit not to the same extent than depletion of SLX4 (Figure 6C, S6C). Furthermore, unlike depletion of SLX4, depleting all three nucleases had no impact in response to HU+ATRi (Data not shown). In agreement, we found that mutating the XPF-binding MLR domain of SLX4 only partially reduced the cytotoxicity associated with over-expression of SLX4 in response to HU, compared to mutating the SIMs or the BTB of SLX4 and had no impact in response to HU+ATRi (Figure 6B and S6B). Overall, our data suggest that the SLX4-mediated toxicity in response to replication stress relies primarily on its SUMO E3 ligase activity and only partially on its nuclease associated functions. We found that SUMOylation of XPF has no obvious impact on the endonuclease activity of the XPF-ERCC1 complex suggesting that it regulates XPF-ERCC1 in other ways (Figure S6E). Similarly, we found no stimulation of the SLX1 nuclease when its co-activator SLX4 is SUMOylated (data not shown). Furthermore, we did not notice any obvious change in SUMOylation of XPF and SLX4 in response to DNA damage (Figure S6D). Nevertheless, correlating with an increase in cell survival, we found that SLX4 depletion resulted in a marked decrease in replication-associated DSBs after HU, as judged by γ H2AX induction and direct measurement of chromosome breakage by PFGE (Figure 6D and 6E). Importantly, SLX4, but not SLX4-SIM^{mut}, restored extensive HU-induced chromosome breakage in cells depleted of endogenous SLX4 (Figure 6F). Taken together, our data suggest that the SLX4 SUMO E3 ligase activity is toxic in response to global replication stress by promoting DSBs.

SLX4 localizes at CFS and promotes chromatid breaks and faithful chromosome segregation

In contrast to the situation of global replication stress, we postulated that promotion of DSBs by SLX4 might be beneficial when replication stress is confined to specific genomic loci that are difficult to replicate, such as common fragile sites (CFS). Indeed, MUS81-EME1 and XPF-ERCC1 were shown to localize at CFS during early mitosis and to promote their expression, which are cytologically visible as gaps and breaks in metaphase chromosomes (Naim et al., 2013; Ying et al., 2013). These activities were postulated to prevent major chromosome segregation defects and cell death. In cells treated with a low dose of aphidicolin (APH) to induce CFS expression, SLX4 formed small foci on mitotic chromosomes that co-localized with FANCD2 (Figure 7A and 7B). This strongly suggested that SLX4 localizes at CFS in mitosis since FANCD2 is essentially associated to CFS in mitotic cells previously exposed to low doses of APH (Chan et al., 2009). Both SLX4-UBZ^{mut} and SLX4-SIM^{mut} still colocalized with FANCD2 (Figure S7A) and were also found at telomeres (Figure S7B) showing that interaction with ubiquitin or SUMO is not required for localization of SLX4 at these specific loci. Importantly, SLX4 colocalized with MUS81 or ERCC1 in mitotic cells (Figure 7C) and was required for their localization at CFS (Figure S7C). No defect was seen in cells expressing SLX4-UBZ^{mut} or SLX4-SIM^{mut} (data not shown). Interestingly, SLX4 mitotic foci could be associated with chromatid breaks (Figure 7C) and endogenous SLX4 mitotic foci could also be detected at chromatid gaps or constrictions (Figure S7D). Thus, we next assessed whether SLX4 overexpression (shown above to be detrimental for cell survival) may promote unscheduled chromosome breakage by examining metaphase spreads.

Overexpression of SLX4 and SLX4-UBZ^{mut} strikingly increased the number of metaphases with chromatid breaks and gaps and a high proportion of metaphases exhibited multiple breaks (Figure 7D and S7E). In contrast, overexpression of SLX4-SIM^{mut} had a less dramatic impact on chromosomal stability while SLX4-BTB^{mut} had no effect. Altogether our data suggest that SLX4 localizes at CFS in a SIM-independent manner but promotes cleavage and chromatid breaks in a SIM-dependent manner. Finally, as CFS cleavage by nucleases promotes faithful sister chromatid disjunction (Naim et al., 2013; Ying et al., 2013), we addressed the role of SLX4 in this process in HeLa FIT cells induced with a low dose of Dox compatible with cell survival and in presence or absence of low doses of aphidicolin (APH) to induce CFS expression. As shown in Figure 7E, expression of SLX4-SIM^{mut}, but not SLX4, led to a significant increase in anaphases bridges and lagging chromosomes as well as mitotic catastrophes when CFS expression was induced by APH. A similar trend in cells producing SLX4-SIM^{mut} was observed even in absence of APH. Interestingly, the defects in cells expressing SLX4-SIM^{mut} were similar to the ones observed in SLX4-depleted cells (Figure 7E). Taken together, our results suggest that the SUMO E3 ligase activity of SLX4 is required to deal with the replication and/or segregation of specific genome loci such as the CFS and to maintain genome stability.

DISCUSSION

SLX4, a new type of SUMO E3 ligase?

Our studies reveal that SLX4 is a SUMO E3 ligase or at least an essential component of a multifactorial SUMO E3 ligase. Interestingly, we found that robust SUMO ligase

activity of the immunoprecipitated SLX4 complex relies on salt-labile cofactors, phosphorylation and can be stimulated by DNA. This suggests a more complex scenario than that of SLX4 acting alone as an efficient SUMO E3 ligase and certainly, a challenging scenario for future reconstitution of full SLX4-mediated SUMO-ligase activity with recombinant proteins.

SUMO E3 ligases facilitate the transfer of SUMO from charged UBC9 towards their substrate. Given the direct interaction between SLX4 and XPF, it is most likely that SLX4 promotes the formation of a transient complex between charged UBC9 and XPF. This kind of substrate specificity driven by E3-SUMO interactions is thought to be especially important for SUMOylation at non-consensus lysines (Gareau and Lima, 2010). In line with this, an XPF mutant where we mutated all lysines in consensus SUMOylation sequences (φ Kx(D/E)) was still SUMOylated (data not shown).

SIM(s) are commonly found in SUMO E3 ligases such as RanBP2 and Pc2 and contribute to their ligase activity (Merrill et al., 2010; Reverter and Lima, 2005; Yang and Sharrocks, 2010). Similarly, we show that SLX4 SIMs are also required for its SUMO E3 ligase activity *in vivo* and *in vitro* suggesting that SUMO binding is a critical determinant for the SUMO E3 ligase activity of SLX4. As previously suggested for other SUMO E3 ligases, SLX4 SIMs could help stabilizing its interaction with charged UBC9~SUMO. Accordingly, we found a robust and surprisingly specific SIM-dependent interaction between SLX4 and only UBC9~SUMO. We propose that this remarkable specificity largely contributes to the SUMO E3 ligase activity of SLX4.

We also show that the BTB domain of SLX4 is required for SUMOylation of XPF *in vivo* and *in vitro*. Since the BTB domain contributes to XPF binding, it may act as a

substrate adaptor module like BTB domains do in Cullin3-based ubiquitin E3 ligases (Pintard et al., 2004). Noteworthy, auto-SUMOylation of SLX4 is also greatly impacted by mutations in the BTB domain suggesting that the BTB domain does not only play a role in XPF targeting. Since the BTB domain also mediates SLX4 oligomerization, one possibility might be that SUMOylation of SLX4 and XPF occur *in trans*, on another molecule of SLX4 and its associated XPF partner. Noteworthy, mutation of the BTB domain dramatically impairs both SLX4 and XPF SUMOylation *in vivo* but to a lesser extent *in vitro* (compare Figure 2 and Figure 4). This may reflect that *in vitro* SLX4 dimerization becomes dispensable for its SUMO E3 ligase activity due to high local protein concentrations. Whether SLX4 defines a novel class of SUMO E3 ligases structured around the BTB-domain awaits the identification of additional BTB-proteins with SUMO-E3 ligase activity. Interestingly, as we were finalizing our study, Slx4 was reported to be necessary in *S. cerevisiae* for SUMOylation of Rad1^{XPF} by Siz1 and Siz2 SUMO E3 ligases (Sarangi et al., 2014). Our results show that evolution has provided the human protein with the ability to directly SUMOylate XPF and that this relies on the acquisition of the BTB domain absent in the yeast protein.

SLX4 and its SUMO-related functions in response to replication stress: The good, the bad and the evil...

We provide evidence that SLX4 and its SUMO-related functions contribute to the maintenance of CFS. Expression of CFS was recently shown to result from the action of MUS81-EME1 and XPF-ERCC1, presumably on late replication intermediates at under-replicated CFS in mitosis, and to be necessary for proper chromosome

segregation and genome stability (Naim et al., 2013; Ying et al., 2013). We propose that in response to replication stress limited to specific genomic loci such as CFS and other under-replicated loci, the SUMO E3 ligase activity of SLX4 promotes, by means that remain to be elucidated, a targeted action of its endonuclease partners. However, while promoting the action of its endonuclease partners at specific genomic loci may contribute to genome stability, promoting their action on a genome wide scale could have dire consequences. In line with this, we found that overexpression of SLX4 induces extensive chromatid breakage and is cytotoxic. Further suggesting that the SUMO E3 ligase activity of SLX4 promotes DNA cleavage, SIMs and BTB mutations reduced or nearly abolished, respectively, chromatid breakage and cytotoxicity. Furthermore, the danger associated with unscheduled SLX4 SUMO-related functions exerted on a genome wide scale was exacerbated when cells overexpressing SLX4 underwent chronic (HU) or acute (HU + ATRi) replication stress. SLX4 promotes HU-induced DSBs, enhancing the cytotoxicity of replication stress imposed by HU. Remarkably, this entirely relies on its SIMs but is only partially mediated through SLX1 and XPF-ERCC1. Furthermore, SUMOylation of XPF does not appear to modulate the nuclease activity of the XPF-ERCC1 complex. Acute replication stress induced by combined HU (or APH) and ATRi treatment results in extensive fork collapse (Couch et al., 2013; Ragland et al., 2013) that depends on SLX4 but not on MUS81 (Couch et al., 2013). Interestingly, we found that the toxicity mediated by SLX4 in response to HU+ATRi treatment entirely relies on its SUMO-related functions but not on its endonuclease-associated functions. Future work will be needed to determine precisely how the SUMO E3 ligase activity of the SLX4 complex is toxic in response to global replication stress independently of its

associated nucleases. Noteworthy, in yeast Slx4 appears to have functions in replication stress response that are independent of its nuclease partners. For instance, Slx4's interactions with Rad1^{XPF}-Rad10^{ERCC1} and the Rtt107 scaffold are mutually exclusive (Flott et al., 2007). The Slx4-Rtt107 complex has anti-checkpoint functions at replication-induced lesions that rely on its interaction with Dpb11^{TOPBP1} and phosphorylated histone H2A (Ohouo et al., 2013). Interestingly, Rtt107 itself interacts the Smc5-6 complex which includes the Mms21 SUMO E3 ligase (Ohouo et al., 2010). It is tempting to speculate that in human cells the SUMO E3 ligase activity of the human SLX4 complex, which we found to be independent of MMS21, fulfills similar functions to those fulfilled by Slx4 in complex with Rtt107 and Smc5-6 in yeast.

An intriguing aspect of our findings is the toxic role of human SLX4 in response to HU and HU+ATRi. This may indicate that in metazoa SLX4 is part of a pathway that eliminates cells undergoing acute replication stress, thereby favoring genome stability at the organismal level (Figure 7F). Analogous roles were previously proposed for MUS81 and the FBH1 helicase (Fugger et al., 2013; Jeong et al., 2013). Following replication stress induced for example by oncogene activation, SLX4 may contribute to a sustained DNA Damage Response that is necessary to establish oncogene induced senescence (OIS), which constitutes an early barrier to tumorigenesis (Bartek et al., 2012). Importantly, recent studies showed that nucleotide pool depletion induced by oncogene activation favours OIS and is also a tumour-suppressive mechanism (Aird and Zhang, 2014). Overall, our experiments using HU-induced nucleotide pool depletion suggest that loss of the SLX4 tumour suppressor might favour oncogenesis by helping precancerous or cancer cells escape OIS.

While SLX4 is likely to be required for the stability of specific loci such as the CFS, our results also suggest that over-activation or misregulation of SLX4 might also constitute a threat by promoting chromosomal instability and in this view, SLX4 could therefore be considered as oncogenic under some circumstances (Figure 7F). Future studies aiming at understanding the consequences of SLX4 overexpression or misregulation of the SUMO E3 ligase activity of SLX4 will help further clarify our understanding of the multifaceted functions of human SLX4.

Ubiquitin and SUMO differentially control SLX4 functions

Protein SUMOylation is often remarkably promiscuous with protein ubiquitination and has emerged in recent years as a key post-translational modification in genome maintenance mechanisms (Jackson and Durocher, 2013; Perry et al., 2008; Ulrich, 2012). In some cases the balance between protein ubiquitination and SUMOylation orchestrates exchange of binding partners and triggers alternative pathways.

Here we show that the SUMO-dependent functions of SLX4, which impact on replication stress outcome and genome stability, are totally independent of the UBZ4 mediated ubiquitin-binding properties of SLX4 and are dispensable for ICL repair.

Therefore, we propose that ubiquitination and SUMOylation differentially control SLX4 and XPF functions in ICL repair and other sources of replication stress that originate at loci that replicate late and/or that are difficult to replicate such as CFS (Figure 7F). Furthermore, both SLX4 and XPF are FA proteins (Bogliolo et al., 2013; Kashiyama et al., 2013; Kim et al., 2011; Stoepker et al., 2011). Accumulating evidence indicates that the FA pathway not only promotes replication-coupled ICL repair but also fulfills important functions in signaling other kinds of replication-

mediated DNA damage induced by oncogene activation and/or challenged replication of fragile sites (Constantinou, 2012; Moldovan and D'andrea, 2012). In this regard, our findings that SLX4 mediates SUMOylation of both XPF and itself, and that its SUMO-dependent functions impact on replication stress outcome may be particularly relevant for understanding the molecular links between the FA pathway and the general replication stress response.

Overall, the discovery that SLX4 is more than a scaffold and that it plays an active role in post-translationally modifying at least one of its partners, opens a broad and fascinating new field of investigation to further understand the molecular mechanisms that underlie the elaborate regulatory functions of SLX4 and their importance in maintaining genome stability and preventing human disease.

EXPERIMENTAL PROCEDURES

FIT inducible cell lines

To generate stably expressing inducible cells producing YFP or FLAG-HA tagged versions of SLX4, Flp-In TRex (FIT₀) parental cell lines - previously cultured in Zeocin (100 µg/ml [Invitrogen]) to maintain the genomic FRT site- were co-transfected with plasmid encoding the Flp recombinase and the pDEST-YFP or FHA version of SLX4 or mutant forms of SLX4.

***In vivo* SUMOylation**

U2OS or HeLa cells were transfected with His-SUMO1+UBC9 or His-SUMO3+UBC9. At the time of transfection, robust overexpression of exogenous SLX4 was induced with doxycycline (Sigma). Cells were collected 24 h later and cell pellets were either frozen at -80°C for subsequent analysis or directly lysed in denaturing urea buffer before His-pulldown with a Co⁺⁺ charged Talon resin (Clontech)

***Ex vivo/in vitro* SUMOylation assay**

Ex vivo/in vitro SUMOylation assays were performed with YFP epitope-tagged SLX4 complexes purified from either HeLa FIT₀ cells transiently transfected with pDEST-YFP-SLX4 or inducible stable HeLa cell lines stably expressing YFP-SLX4 (10 ng/ml of dox) incubated with recombinant SAE1/SAE2, UBC9, SUMO2, +/- ATP.

Immunofluorescence

Immunofluorescence experiments were performed on cells grown on glass coverslips as described previously (Naim and Rosselli, 2009).

FIGURE LEGENDS

Figure 1. SLX4 is a SUMO binding protein

(A) Sequence alignments of SLX4 SIMs among various organisms.

(B) *In vitro* interaction between recombinant His-MBP-tagged fragments of SLX4 and purified SUMO3 chains. Blots were extracted from the same film exposure of a single gel.

(C) Same as (B). Mutagenesis of aliphatic residues in each SIM were performed on SLX4₁₀₄₃₋₁₄₆₂.

(D) Co-immunoprecipitation of SUMOylated proteins with FLAG-tagged WT or SIM mutants of SLX4 from HeLa cells.

Figure 2. SLX4 promotes XPF SUMOylation *in vivo*

(A) U2OS FIT₀ or YFP-SLX4 cells were treated with Doxycycline (Dox) (1 μ g/ml), transfected with His-SUMO1 or His-SUMO3 along with UBC9. Cells were lysed in denaturing buffer containing 8 M Urea and His-SUMOylated proteins were purified on a Co⁺⁺ column before analysis by Western blot (WB) with SLX4 and XPF antibodies. SLX4 protein is prone to breakage during sonication combined with denaturing lysis explaining the smeary migration pattern of SUMOylated SLX4. Blots were extracted from the same film exposure of a single gel.

(B) U2OS YFP-SLX4 cells were transfected with CTRL siRNA or siRNAs targeting both endogenous and exogenous (siSLX4) SLX4 and were handled as in (A).

(C) Same as in (A) but SUMOylation of SLX4 and XPF was assessed in Dox-treated U2OS FIT₀ versus F-HA SLX4, SLX4-UBZ^{mut} and SLX4-SIM^{mut}.

(D) FLAG-SLX4 WT or harbouring mutations in its MLR or BTB domains was transiently expressed in 293 cells followed by FLAG immunoprecipitation and analysis of co-immunoprecipitated endogenous XPF.

(E) Same as in (C) but SUMOylation of SLX4 and XPF was assessed in Dox-treated U2OS FIT₀ versus YFP-SLX4, SLX4-MLR^{mut} and SLX4-BTB^{mut}.

Figure 3. SLX4 SIM1 and SIM2 specifically interact with the charged UBC9~SUMO E2 enzyme

(A) F-HA-tagged UBC9 was transiently expressed in HeLa YFP-SLX4 or SLX4-SIM^{mut} cells before cell lysis and immunoprecipitation of F-HA-UBC9. Co-immunoprecipitated YFP-SLX4 was analysed by Western blot.

(B) Experimental procedure for the two-step analysis of UBC9/SLX4 interaction used in Figure 3 (C-E). A SUMOylation reaction with recombinant E1, UBC9 and SUMO2 was first performed before incubation for 1 h at RT with His-MBP-SLX4₆₈₄₋₁₂₀₆ immobilized on an amylose resin, as detailed in material and methods.

(C) Unbound and bound fractions of both SLX4 and SLX4-SIM^{mut} were analysed by SDS-PAGE either without reducing the sample (-DTT) to preserve the UBC9~SUMO thioester bond (upper gel) or after reducing the samples (+DTT) (lower gels). UBC9_{SUMO2} represents SUMOylated UBC9 (isopeptide bond). (*) indicates a band that corresponds to a UBC9 dimer that runs close to UBC9~SUMO and disappears when samples are reduced before SDS-PAGE or when ATP is added to the SUMO ligation reaction.

(D) Same as in (C) but with SLX4₆₈₄₋₁₂₀₆ harbouring mutations in negatively charged residues (ED mutants) in SIM 1 and SIM 2.

(E) Same as in (C) but using SLX4₆₈₄₋₁₂₀₆ and recombinant UBC9 WT, C93S (catalytically inactive) and UBC9 basic patch mutants K65A and K74A. Note that the UBC9 dimer (*) of C93S does not disappear when ATP is added to the SUMO ligation reaction. UBC9 K65A and K74A are charged and SUMOylated similarly to WT UBC9 but are impaired in SLX4 interaction.

(F) Schematic representation of SLX4 interaction with charged UBC9~SUMO. Left: no (or weak) interaction of SLX4 with free SUMO or unmodified UBC9. Middle: Robust and specific interaction with charged UBC9~SUMO involving both SUMO-SIM recognition requiring SLX4 SIM1 aliphatic residues (data not shown) and electrostatic interactions between negative charges in SIM1 and SIM2 and the basic patch of UBC9. Right: the SUMO moiety of UBC9_{SUMO}, cristallized by Knipscheer et al. (Knipscheer et al., 2008), is spatially far from the basic patch of UBC9 and thus probably cannot allow interaction with SLX4.

Figure 4. The SLX4 complex has SUMO E3 ligase activity.

(A) Schematic diagram for the *ex vivo/in vitro* SUMOylation assay.

(B) YFP-SLX4 complexes were immunoprecipitated from stable inducible HeLa YFP-SLX4 cells and incubated with recombinant E1, E2, SUMO2 +/- ATP at 37°C for the indicated time.

(C) SUMOylation assays performed as in (B) except that YFP-SLX4 complexes were immunoprecipitated from HeLa FIT₀ cells transiently expressing YFP-SLX4, SIM^{mut} or BTB^{mut}. The kinetic analyses reveal a defect of SUMOylation with SLX4 SIM^{mut} and BTB^{mut} complexes.

(D) SUMOylation assay with the indicated UBC9 mutants and YFP-SLX4 complexes immunoprecipitated as in (B) and incubated with recombinant E1, SUMO2 and ATP at 37°C.

(E) Same as in (B) except that transiently expressed SLX4 complexes purified from HeLa cells were washed either with a standard 150 mM NaCl Wash buffer (as in B, C and D) or with a 500 mM NaCl Wash buffer before *in vitro* SUMOylation assay.

(F) YFP-SLX4 complexes were prepared as in (E) and preincubated at 30°C for 30 min with or without digested or undigested plasmid DNA before a 60 min SUMO ligase reaction.

(G) Left Panel: YFP-SLX4, SIM^{mut} and BTB^{mut} complexes immunoprecipitated as in (C) and washed with a standard 150 mM NaCl Wash buffer were preincubated at 30°C for 30 min with or without digested plasmid DNA before a 30 min SUMO ligase reaction. Right Panel: 500 mM NaCl washed YFP-SLX4 IP preincubated with or without digested DNA before a 30 min SUMO ligase reaction.

(H) YFP-SLX4 complexes immunoprecipitated as in (B) were preincubated with or without active or inactivated lambda phosphatase at 30°C for 60 min before a 30 min SUMO ligase reaction.

Figure 5. SIM-dependent functions of SLX4 are not required for ICL repair but contribute to cellular toxicity induced by SLX4 overexpression

(A) Representative images of colony survival assays performed in U2OS FIT₀ cells and U2OS YFP-SLX4 cells grown under various concentrations of Dox.

(B) Left: quantitative measurement of colony survival of U2OS FIT₀ cells, YFP-SLX4, UBZ^{mut}, SIM^{mut}, UBZ/SIM^{mut} and BTB^{mut} cells under constant treatment with Dox.

Values represent means and SEMs of at least three independent experiments. Right: representative WB showing expression levels of the various YFP-SLX4 constructs.

(C) Mitomycin C (MMC) complementation assays. U2OS cells expressing various constructs of YFP-SLX4 were transfected with siRNA targeting endogenous SLX4 (siSLX4^{endo}), seeded at low density with 2 ng/ml Dox for 24 h and then treated with 75 or 300 ng/ml MMC for 1 h before PBS wash and release into medium containing 1 ng/ml Dox. Values represent the means and SEM from 3 to 8 independent experiments.

Figure 6. HU-induced toxicity is mediated by the SUMO-related functions of SLX4

(A) HeLa cells transfected twice with siRNAs CTRL or siSLX4^{endo} before seeding at low density with 1 ng/ml Dox. Hydroxyurea (HU) was added the next day at 500 μ M for 24 h. Cells were then washed and released into fresh medium with 1 ng/ml Dox.

(B) Same as in (A) but cells were treated for 24 h with a low dose of HU (100 μ M) combined with the ATR inhibitor (ATRi) VE-821 at 1 μ M.

(C) Same as in (A) and (B), except that HeLa SLX4 cells were transfected with siCTRL or siRNAs targeting the nucleases associated to SLX4. As a control, FIT₀ cells were transfected with siSLX4^{endo} as a reference for HU resistance.

(D) HeLa FIT₀ cells transfected twice with siCTRL or siSLX4^{endo} were treated with 500 μ M HU for 24 h, harvested or eventually released for 2 or 4 h before analysis of RPA32 and H2AX phosphorylations by western blot.

(E) Pulse-Field Gel Electrophoresis (PFGE). HeLa FIT₀ cells transfected twice with siCTRL or siSLX4^{endo} were treated with 500 μ M or 2 mM of HU for 24 h before cells

were embedded in low-melting agarose, treated with proteinase K and subsequent PFGE analysis. Intact chromosomes are stacked in the wells while fragmented DNA can further migrate.

(F) Quantification of fragmented DNA detected by PFGE after a 500 μ M HU treatment of FIT₀ cells and cells expressing SLX4 or SLX4-SIM^{mut} and transfected with siCTRL or siSLX4^{endo} as indicated. Values represent the means and SEM from 3 independent experiments.

Figure 7. SLX4 localizes at CFS and promotes chromatid breakage to promote faithful chromosome segregation

(A) Representative images of co-localization of FANCD2 and SLX4 in prophase and metaphase from APH-treated HeLa F-HA SLX4 cells (Dox: 0.5 μ g/ml ; APH: 0.3 μ M) stained with FANCD2 (red in the merged image) and HA (green in the merged image) specific antibodies.

(B) Representative images of co-localization of FANCD2 and YFP-SLX4 on mitotic chromosomes from APH-treated HeLa YFP-SLX4 or SIM^{mut} cells (Dox: 0.5 μ g/ml) stained with a FANCD2 specific antibody.

(C) Co-localization of YFP-SLX4 with ERCC1 and MUS81 at chromatid breaks in mitosis.

(D) Quantification of metaphase with gap(s) and break(s) among total metaphases in U2OS FIT₀, YFP-SLX4, YFP-SIM^{mut}, YFP-UBZ^{mut} and YFP-BTB^{mut} cells treated with 10 ng/ml Dox for 48 h before addition of colchicine and metaphase preparation. Data represent mean +/- SEM.

E) Upper panels: representative anaphase cells scored in phenotypic analysis: a regular anaphase (*i*), and irregular anaphases presenting lagging chromosomes (*ii*), chromosome bridges (*iii*), or segregation failure (*iv*), are shown. Scale bars= 10 μm . Lower panel: quantification of the chromosome segregation defects in control HeLa FIT₀ cells and cells expressing YFP-SLX4 or YFP-SLX4-SIM^{mut} transfected with siCTRL or siSLX4 as indicated (Dox: 1 ng/ml). The mean values \pm s.d. of at least 3 independent experiments are indicated. Around 50 anaphases were scored for each experiment and condition. Data were analysed with unpaired Student's *t*-test. * $P < 0.05$; ** $P < 0.01$; compared to HeLa FIT₀ siCTRL.

F) Model summarizing our findings and speculations discussed in the text.

REFERENCES

- Aird, K.M., and Zhang, R. (2014). Nucleotide metabolism, oncogene-induced senescence and cancer. *Cancer Lett.*
- Andersen, S.L., Bergstralh, D.T., Kohl, K.P., LaRocque, J.R., Moore, C.B., and Sekelsky, J. (2009). *Drosophila* MUS312 and the vertebrate ortholog BTBD12 interact with DNA structure-specific endonucleases in DNA repair and recombination. *Mol Cell* *35*, 128–135.
- Ashton, T.M., Mankouri, H.W., Heidenblut, A., McHugh, P.J., and Hickson, I.D. (2011). Pathways for Holliday junction processing during homologous recombination in *Saccharomyces cerevisiae*. *Mol Cell Biol* *31*, 1921–1933.
- Bartek, J., Mistrik, M., and Bartkova, J. (2012). Thresholds of replication stress signaling in cancer development and treatment. *Nat Struct Mol Biol* *19*, 5–7.
- Bogliolo, M., Schuster, B., Stoepker, C., Derkunt, B., Su, Y., Raams, A., Trujillo, J.P., Minguillón, J., Ramírez, M.J., Pujol, R., et al. (2013). Mutations in ERCC4, encoding the DNA-repair endonuclease XPF, cause Fanconi anemia. *Am. J. Hum. Genet.* *92*, 800–806.
- Castor, D., Nair, N., Déclais, A.-C., Lachaud, C., Toth, R., Macartney, T.J., Lilley, D.M.J., Arthur, J.S.C., and Rouse, J. (2013). Cooperative Control of Holliday Junction Resolution and DNA Repair by the SLX1 and MUS81-EME1 Nucleases. *Mol Cell* *52*, 221-233.
- Chan, K.L., Palmai-Pallag, T., Ying, S., and Hickson, I.D. (2009). Replication stress induces sister-chromatid bridging at fragile site loci in mitosis. *Nat Cell Biol* *11*, 753–760.
- Constantinou, A. (2012). Rescue of replication failure by Fanconi anaemia proteins. *Chromosoma* *121*, 21–36.
- Couch, F.B., Bansbach, C.E., Driscoll, R., Luzwick, J.W., Glick, G.G., Betous, R., Carroll, C.M., Jung, S.Y., Qin, J., Cimprich, K.A., et al. (2013). ATR phosphorylates SMARCAL1 to prevent replication fork collapse. *Genes Dev* *27*, 1610–1623.
- Coulon, S., Gaillard, P.-H.L., Chahwan, C., McDonald, W.H., Yates, J.R., and Russell, P. (2004). Slx1-Slx4 are subunits of a structure-specific endonuclease that maintains ribosomal DNA in fission yeast. *Mol Biol Cell* *15*, 71–80.
- Crossan, G.P., van der Weyden, L., Rosado, I.V., Langevin, F., Gaillard, P.-H.L., McIntyre, R.E., Sanger Mouse Genetics Project, Gallagher, F., Kettunen, M.I., Lewis, D.Y., et al. (2011). Disruption of mouse Slx4, a regulator of structure-specific nucleases, phenocopies Fanconi anemia. *Nat Genet* *43*, 147–152.
- Douwel, D.K., Boonen, R.A.C.M., Long, D.T., Szybowska, A.A., Räschle, M., Walter, J.C., and Knipscheer, P. (2014). XPF-ERCC1 Acts in Unhooking DNA Interstrand Crosslinks in Cooperation with FANCD2 and FANCP/SLX4. *Mol Cell* *54*, 460-471.

- Fekairi, S., Scaglione, S., Chahwan, C., Taylor, E.R., Tissier, A., Coulon, S., Dong, M.-Q., Ruse, C., Yates, J.R., Russell, P., et al. (2009). Human SLX4 is a Holliday junction resolvase subunit that binds multiple DNA repair/recombination endonucleases. *Cell* *138*, 78–89.
- Flott, S., Alabert, C., Toh, G.W., Toth, R., Sugawara, N., Campbell, D.G., Haber, J.E., Pasero, P., and Rouse, J. (2007). Phosphorylation of Slx4 by Mec1 and Tel1 regulates the single-strand annealing mode of DNA repair in budding yeast. *Mol Cell Biol* *27*, 6433–6445.
- Fugger, K., Chu, W.K., Haahr, P., Nedergaard Kousholt, A., Beck, H., Payne, M.J., Hanada, K., Hickson, I.D., and Storgaard Sørensen, C. (2013). FBH1 co-operates with MUS81 in inducing DNA double-strand breaks and cell death following replication stress. *Nat Commun* *4*, 1423.
- Gareau, J.R., and Lima, C.D. (2010). The SUMO pathway: emerging mechanisms that shape specificity, conjugation and recognition. *Nat Rev Mol Cell Biol* *11*, 861–871.
- Garner, E., Kim, Y., Lach, F.P., Kottemann, M.C., and Smogorzewska, A. (2013). Human GEN1 and the SLX4-Associated Nucleases MUS81 and SLX1 Are Essential for the Resolution of Replication-Induced Holliday Junctions. *Cell Rep* *5*, 207-215.
- Hodskinson, M.R.G., Silhan, J., Crossan, G.P., Garaycochea, J.I., Mukherjee, S., Johnson, C.M., Schärer, O.D., and Patel, K.J. (2014). Mouse SLX4 Is a Tumor Suppressor that Stimulates the Activity of the Nuclease XPF-ERCC1 in DNA Crosslink Repair. *Mol Cell* *54*, 472-484.
- Jackson, S.P., and Durocher, D. (2013). Regulation of DNA Damage Responses by Ubiquitin and SUMO. *Mol Cell* *49*, 795–807.
- Jeong, Y.T., Rossi, M., Cermak, L., Saraf, A., Florens, L., Washburn, M.P., Sung, P., Schildkraut, C.L., and Pagano, M. (2013). FBH1 promotes DNA double-strand breakage and apoptosis in response to DNA replication stress. *J Cell Biol* *200*, 141–149.
- Kaliraman, V., and Brill, S.J. (2002). Role of SGS1 and SLX4 in maintaining rDNA structure in *Saccharomyces cerevisiae*. *Curr Genet* *41*, 389–400.
- Kashiyama, K., Nakazawa, Y., Pilz, D.T., Guo, C., Shimada, M., Sasaki, K., Fawcett, H., Wing, J.F., Lewin, S.O., Carr, L., et al. (2013). Malfunction of nuclease ERCC1-XPF results in diverse clinical manifestations and causes Cockayne syndrome, xeroderma pigmentosum, and Fanconi anemia. *Am. J. Hum. Genet.* *92*, 807–819.
- Kerscher, O. (2007). SUMO junction-what's your function? New insights through SUMO-interacting motifs. *EMBO Rep* *8*, 550–555.
- Kim, Y., Lach, F.P., Desetty, R., Hanenberg, H., Auerbach, A.D., and Smogorzewska, A. (2011). Mutations of the SLX4 gene in Fanconi anemia. *Nat Genet* *43*, 142–146.

- Kim, Y., Spitz, G.S., Vaturi, U., Lach, F.P., Auerbach, A.D., and Smogorzewska, A. (2013). Regulation of multiple DNA repair pathways by the Fanconi anemia protein SLX4. *Blood* *121*, 54–63.
- Knipscheer, P., Flotho, A., Klug, H., Olsen, J.V., van Dijk, W.J., Fish, A., Johnson, E.S., Mann, M., Sixma, T.K., and Pichler, A. (2008). Ubc9 sumoylation regulates SUMO target discrimination. *Mol Cell* *31*, 371–382.
- Lin, D.-Y., Huang, Y.-S., Jeng, J.-C., Kuo, H.-Y., Chang, C.-C., Chao, T.-T., Ho, C.-C., Chen, Y.-C., Lin, T.-P., Fang, H.-I., et al. (2006). Role of SUMO-Interacting Motif in Daxx SUMO Modification, Subnuclear Localization, and Repression of Sumoylated Transcription Factors. *Mol Cell* *24*, 341–354.
- Melchior, F. (2003). SUMO: ligases, isopeptidases and nuclear pores. *Trends Biochem Sci* *28*, 612–618.
- Merrill, J.C., Melhuish, T.A., Kagey, M.H., Yang, S.-H., Sharrocks, A.D., and Wotton, D. (2010). A role for non-covalent SUMO interaction motifs in Pc2/CBX4 E3 activity. *PLoS ONE* *5*, e8794.
- Mohideen, F., Capili, A.D., Bilimoria, P.M., Yamada, T., Bonni, A., and Lima, C.D. (2009). A molecular basis for phosphorylation-dependent SUMO conjugation by the E2 UBC9. *Nat Struct Mol Biol* *16*, 945–952.
- Moldovan, G.-L., and D'andrea, A.D. (2012). To the rescue: the fanconi anemia genome stability pathway salvages replication forks. *Cancer Cell* *22*, 5–6.
- Munoz, I.M., Hain, K., Déclais, A.-C., Gardiner, M., Toh, G.W., Sanchez-Pulido, L., Heuckmann, J.M., Toth, R., Macartney, T., Eppink, B., et al. (2009). Coordination of structure-specific nucleases by human SLX4/BTBD12 is required for DNA repair. *Mol Cell* *35*, 116–127.
- Naim, V., and Rosselli, F. (2009). The FANCD1 pathway and BLM collaborate during mitosis to prevent micro-nucleation and chromosome abnormalities. *Nat Cell Biol* *11*, 761–768.
- Naim, V., Wilhelm, T., Debatisse, M., and Rosselli, F. (2013). ERCC1 and MUS81-EME1 promote sister chromatid separation by processing late replication intermediates at common fragile sites during mitosis. *Nat Cell Biol* *15*, 1008–1015.
- Ohouo, P.Y., Bastos de Oliveira, F.M., Almeida, B.S., and Smolka, M.B. (2010). DNA damage signaling recruits the Rtt107-Slx4 scaffolds via Dpb11 to mediate replication stress response. *Mol Cell* *39*, 300–306.
- Ohouo, P.Y., Bastos de Oliveira, F.M., Liu, Y., Ma, C.J., and Smolka, M.B. (2013). DNA-repair scaffolds dampen checkpoint signalling by counteracting the adaptor Rad9. *Nature* *493*, 120–124.
- Perez-Torrado, R., Yamada, D., and Defossez, P.-A. (2006). Born to bind: the BTB protein-protein interaction domain. *Bioessays* *28*, 1194–1202.

- Perry, J.J.P., Tainer, J.A., and Boddy, M.N. (2008). A SIM-ultaneous role for SUMO and ubiquitin. *Trends Biochem Sci* *33*, 201–208.
- Pintard, L., Willems, A., and Peter, M. (2004). Cullin-based ubiquitin ligases: Cul3–BTB complexes join the family. *Embo J* *23*, 1681–1687.
- Ragland, R.L., Patel, S., Rivard, R.S., Smith, K., Peters, A.A., Bielinsky, A.K., and Brown, E.J. (2013). RNF4 and PLK1 are required for replication fork collapse in ATR-deficient cells. *Genes Dev* *27*, 2259–2273.
- Reverter, D., and Lima, C.D. (2005). Insights into E3 ligase activity revealed by a SUMO–RanGAP1–Ubc9–Nup358 complex. *Nat Cell Biol* *435*, 687–692.
- Sarangi, P., Bartosova, Z., Altmannova, V., Holland, C., Chavdarova, M., Lee, S.E., Krejci, L., and Zhao, X. (2014). Sumoylation of the Rad1 nuclease promotes DNA repair and regulates its DNA association. *Nucleic Acids Res.* *42*, 6393-6404.
- Seeler, J.-S., and Dejean, A. (2003). Nuclear and unclear functions of SUMO. *Nat Rev Mol Cell Biol* *4*, 690–699.
- Stoepker, C., Hain, K., Schuster, B., Hilhorst-Hofstee, Y., Rooimans, M.A., Steltenpool, J., Oostra, A.B., Eirich, K., Korthof, E.T., Nieuwint, A.W.M., et al. (2011). SLX4, a coordinator of structure-specific endonucleases, is mutated in a new Fanconi anemia subtype. *Nat Genet* *43*, 138–141.
- Svendsen, J.M., and Harper, J.W. (2010). GEN1/Yen1 and the SLX4 complex: Solutions to the problem of Holliday junction resolution. *Genes Dev* *24*, 521–536.
- Svendsen, J.M., Smogorzewska, A., Sowa, M.E., O'Connell, B.C., Gygi, S.P., Elledge, S.J., and Harper, J.W. (2009). Mammalian BTBD12/SLX4 assembles a Holliday junction resolvase and is required for DNA repair. *Cell* *138*, 63–77.
- Takahashi, H. (2004). Noncovalent SUMO-1 Binding Activity of Thymine DNA Glycosylase (TDG) Is Required for Its SUMO-1 Modification and Colocalization with the Promyelocytic Leukemia Protein. *Journal of Biological Chemistry* *280*, 5611–5621.
- Toh, G.W.-L., Sugawara, N., Dong, J., Toth, R., Lee, S.E., Haber, J.E., and Rouse, J. (2010). Mec1/Tel1-dependent phosphorylation of Slx4 stimulates Rad1-Rad10-dependent cleavage of non-homologous DNA tails. *DNA Repair (Amst)* *9*, 718–726.
- Ulrich, H.D. (2012). Ubiquitin and SUMO in DNA repair at a glance. *J Cell Sci* *125*, 249–254.
- Vannier, J.-B., Pavicic-Kaltenbrunner, V., Petalcorin, M.I.R., Ding, H., and Boulton, S.J. (2012). RTEL1 dismantles T loops and counteracts telomeric G4-DNA to maintain telomere integrity. *Cell* *149*, 795–806.
- Wan, B., Yin, J., Horvath, K., Sarkar, J., Chen, Y., Wu, J., Wan, K., Lu, J., Gu, P., Yu, E.Y., et al. (2013). SLX4 Assembles a Telomere Maintenance Toolkit by Bridging

Multiple Endonucleases with Telomeres. *Cell Rep* 4, 861–869.

Wechsler, T., Newman, S., and West, S.C. (2011). Aberrant chromosome morphology in human cells defective for Holliday junction resolution. *Nature* 471, 642–646.

Wilson, J.S.J., Tejera, A.M., Castor, D., Toth, R., Blasco, M.A., and Rouse, J. (2013). Localization-Dependent and -Independent Roles of SLX4 in Regulating Telomeres. *Cell Rep* 4, 853–860.

Wu, L., and Hickson, I.D. (2003). The Bloom's syndrome helicase suppresses crossing over during homologous recombination. *Nature* 426, 870–874.

Wyatt, H.D.M., Sarbajna, S., Matos, J., and West, S.C. (2013). Coordinated Actions of SLX1-SLX4 and MUS81-EME1 for Holliday Junction Resolution in Human Cells. *Mol Cell* 52, 234-247.

Yang, S.-H., and Sharrocks, A.D. (2010). The SUMO E3 ligase activity of Pc2 is coordinated through a SUMO interaction motif. *Mol Cell Biol* 30, 2193–2205.

Ying, S., Minocherhomji, S., Chan, K.L., Palmai-Pallag, T., Chu, W.K., Wass, T., Mankouri, H.W., Liu, Y., and Hickson, I.D. (2013). MUS81 promotes common fragile site expression. *Nat Cell Biol* 15, 1001–1007.

SUPPLEMENTAL DATA

Supplemental Data include detailed Supplemental Experimental Procedures and Supplemental figures.

ACKNOWLEDGEMENTS

We thank Pierre-Marie Dehé, Mauro Modesti, Bertrand Llorente, Michelle Debatisse and Orlando Schärer for fruitful discussions throughout the course of this study as well as Pierre-Marie Dehé and Jesse Allevinah for their technical help. We are very grateful to Claus Storgaard Sørensen and Kasper Fugger for stimulating discussions as well as technical recommendation for PFGE. We also thank Thomas Bonacci for methodological advice.

“Merci” to Paul Russell and Nick Boddy for their critical reading of the manuscript and encouragements. We are indebted to Palm Silver, Stephen Taylor, Jean-Pierre Quivy and Geneviève Almouzni for FLP-in-TREX inducible cell lines, Jacob Seeler and Anne Dejean for His-SUMO1 and UBC9, Zuzana Horejsi and Simon Boulton for pDEST-FRT-TO plasmid, Patrick Ryan Potts and Hongtao Yu for anti-MMS21 and John Rouse for generously sharing anti-SLX antibodies.

This work was primarily funded by the following grants INCa PLBIO 2012-111, “Teloloop” ANR-1582-30020690, ARC-SF1582, FRM ING 2009 1218198 and SIRIC INCa-DGOS-Inserm 6038s that were awarded to P.-H.L.G. as well as by grants from “La Ligue Contre le Cancer” and SIRIC INCa-DGOS-INSERM 6043 awarded to F.R.. J.-H.G. received a 3 year ARC postdoctoral fellowship. A.T. received a 1 year SSHN fellowship from the French Government.

AUTHOR CONTRIBUTIONS

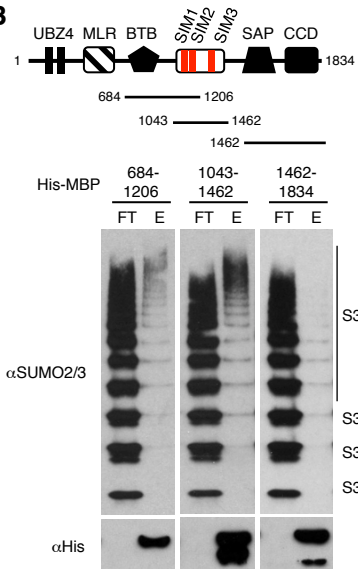
J.-H.G., A.T. and P.-H.L.G conceived the project, with help from E.D. and P.K.. J.-H.G. carried out the biochemical characterization of the SIMs, J.-H.G. carried out all experiments on the in vivo SUMO-binding and in vivo SUMO E3 ligase properties of SLX4 and UBC9/SLX4 interaction. A.T. carried out the ex vivo/in vitro SUMO ligase assays. Colony survival assays were done by J.-H.G and A.T., with technical help from Y.L. and S.S. Metaphase spreads were done by J.-H.G.. Recombinant XPF-ERCC1 was produced by I.K. All experiments related to CFS stability and mitotic defects were designed and performed by V.N. and F.R.. C.C. made the initial *in silico* identification of the SIMs in SLX4. Routine molecular biology experiments were performed by J.-H.G. and S.S.. Most stable inducible cell lines were generated by J.-H.G. with some generated by A.T.. PFGE experiments were performed by A.T. and S.S.. The nuclease assays were performed by S.S.. SS also provided important technical assistance throughout the project for routine analytical experiments. J.-H.G. and P.-H.L.G wrote the paper.

Figure 1

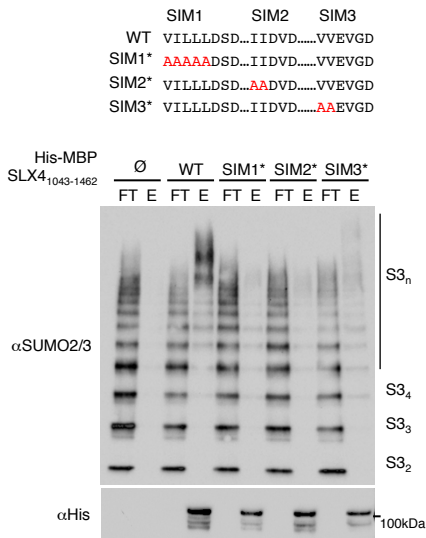
A

	SIM1	SIM2	SIM3
H.sapiens:	EEDEVILLLLDSDEEEL...ELFSIIDVDADQE...	...PAGEVVEVGDSDDEQ	
M.musculus:	KEDEVILLLLDSDEEELH...ELFSVIDVEEDHE...	...AADDVVEVGDSDDEV	
B.taurus:	REDEVILLLLDSDEEEL...EPFSIIDLDAEQE...	...PVSEVVEVEDESEQ	
G.gallus:	KKGDVIVLSSDDEMELE...	...DKSNVSVVEIQDSEG	
X.tropicalis:	QEPDVILLLSSDETEP...	...TSSSVVEVGDSEDDG	
D.rerio:	KQVELIVLSDSDSNEGMD...	...SVEEVVDISRKLSLD	
D.melanogaster:	DDAVVDLLDDEEK...		

B



C



D

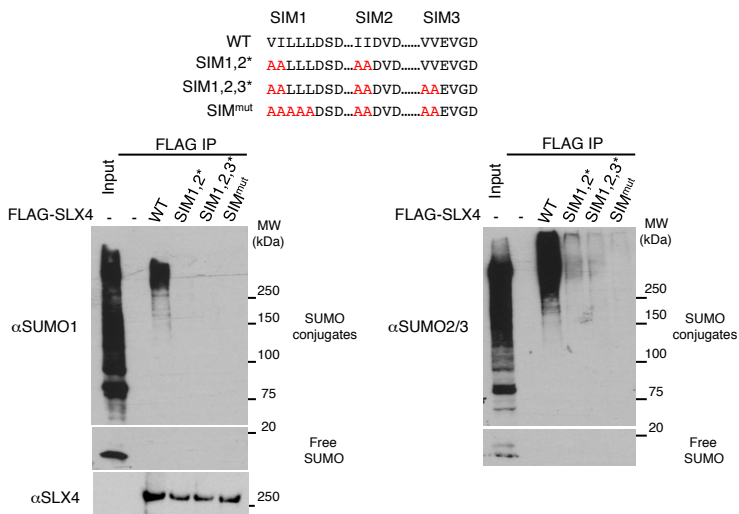


Figure 2

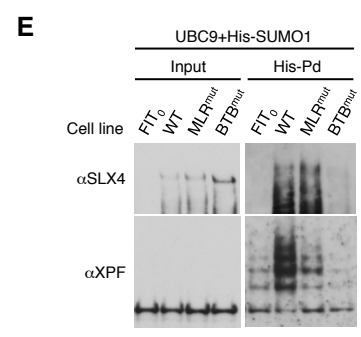
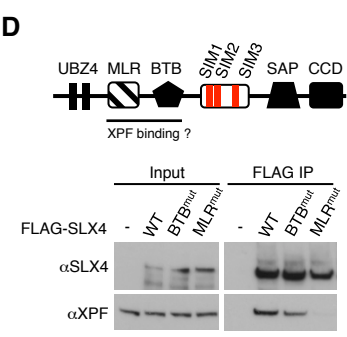
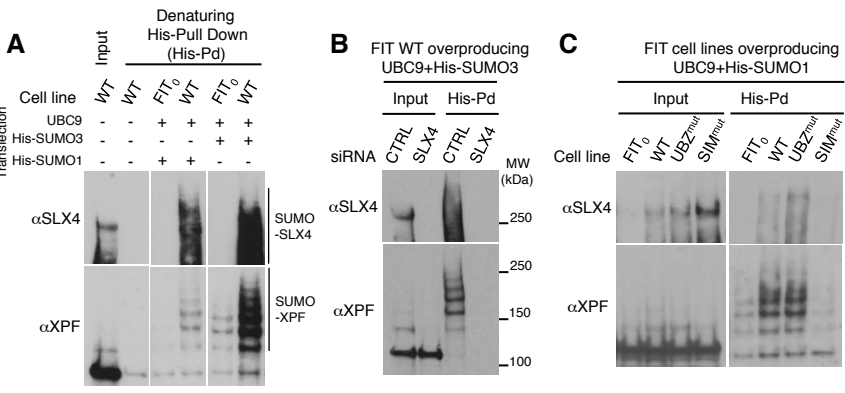
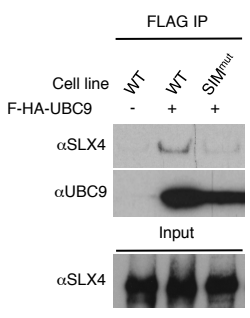
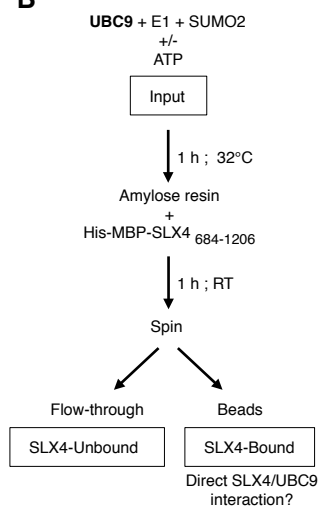


Figure 3

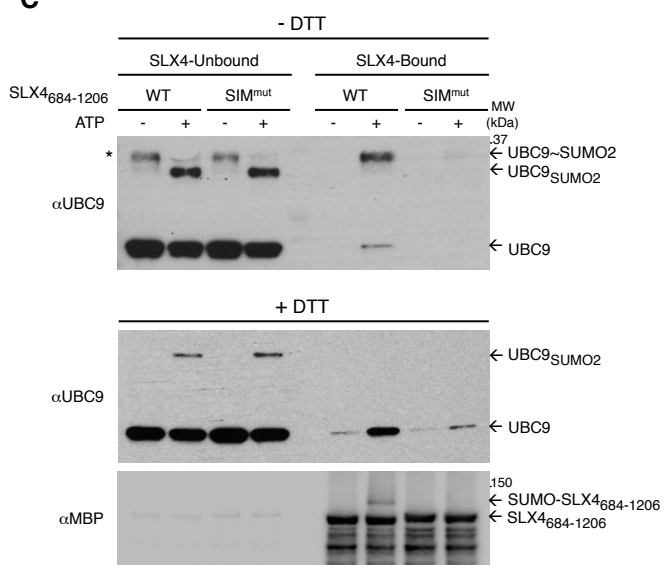
A



B

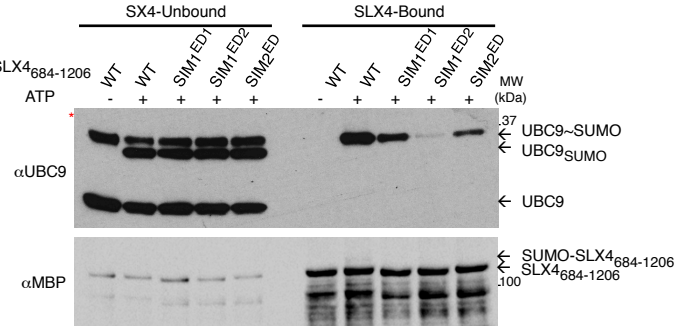


C

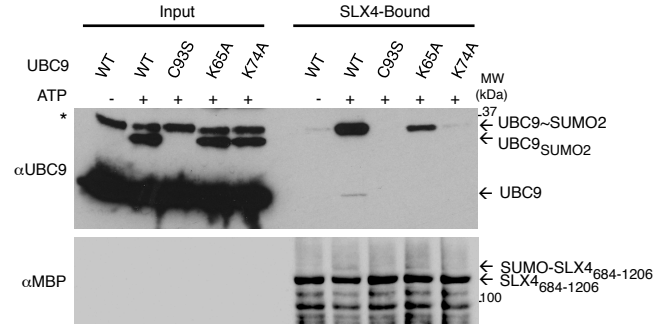


D

SIM1 wt: EEDEVILLLSDEELELE
 SIM1^{ED1}: AAAAVILLLSDEELELE
 SIM1^{ED2}: EEDEVILLASAAALALE
 SIM2 wt: FSIIDVDADQE
 SIM2^{ED}: FSIIAVAAAQA



E



F

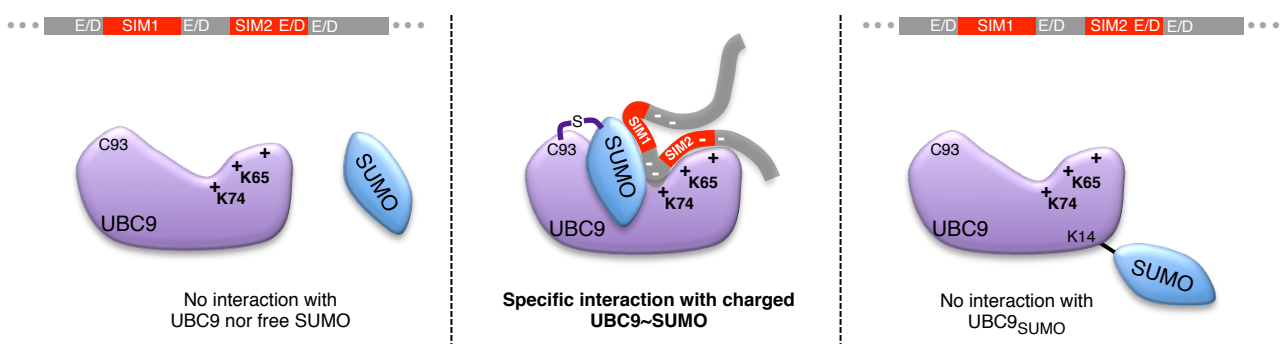
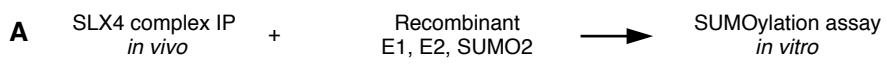
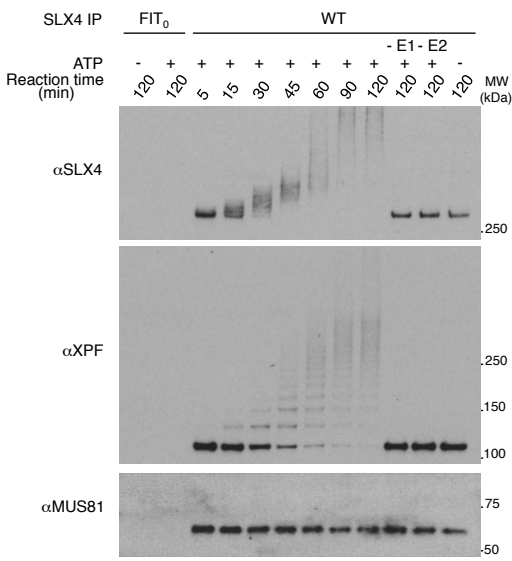


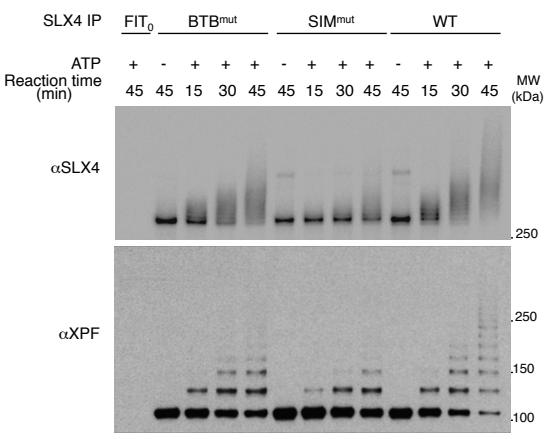
Figure 4



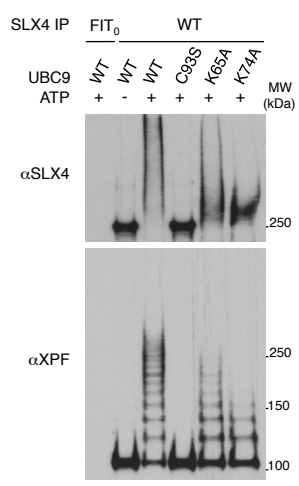
B



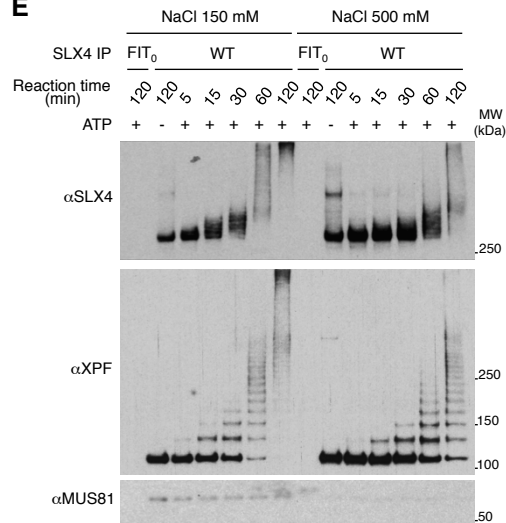
C



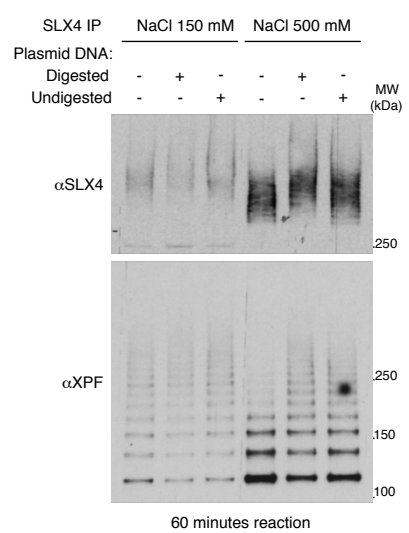
D



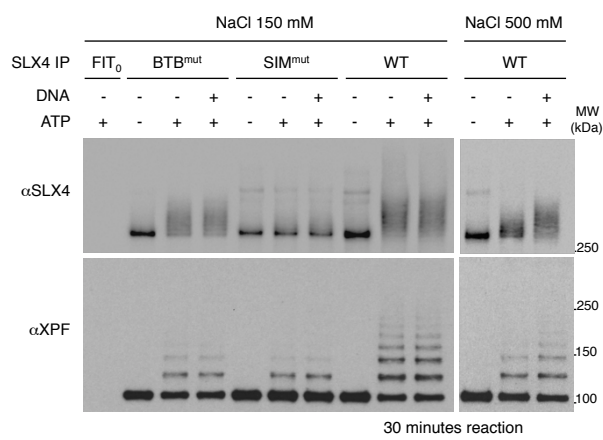
E



F



G



H

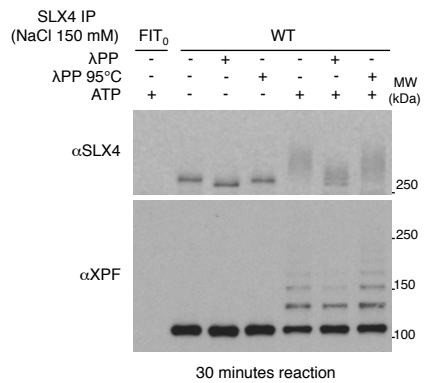
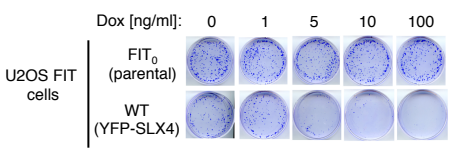
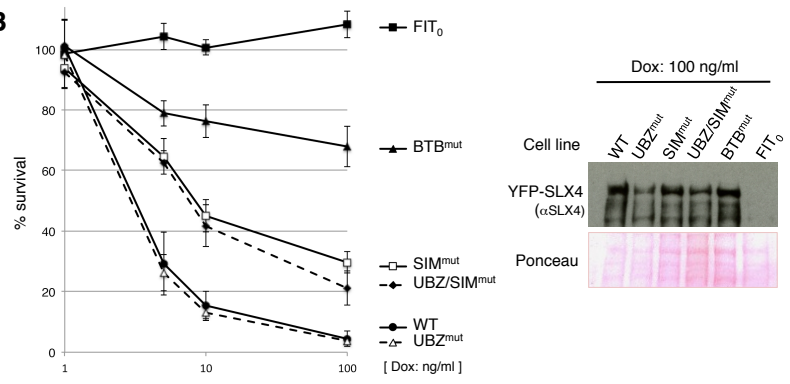


Figure 5

A



B



C

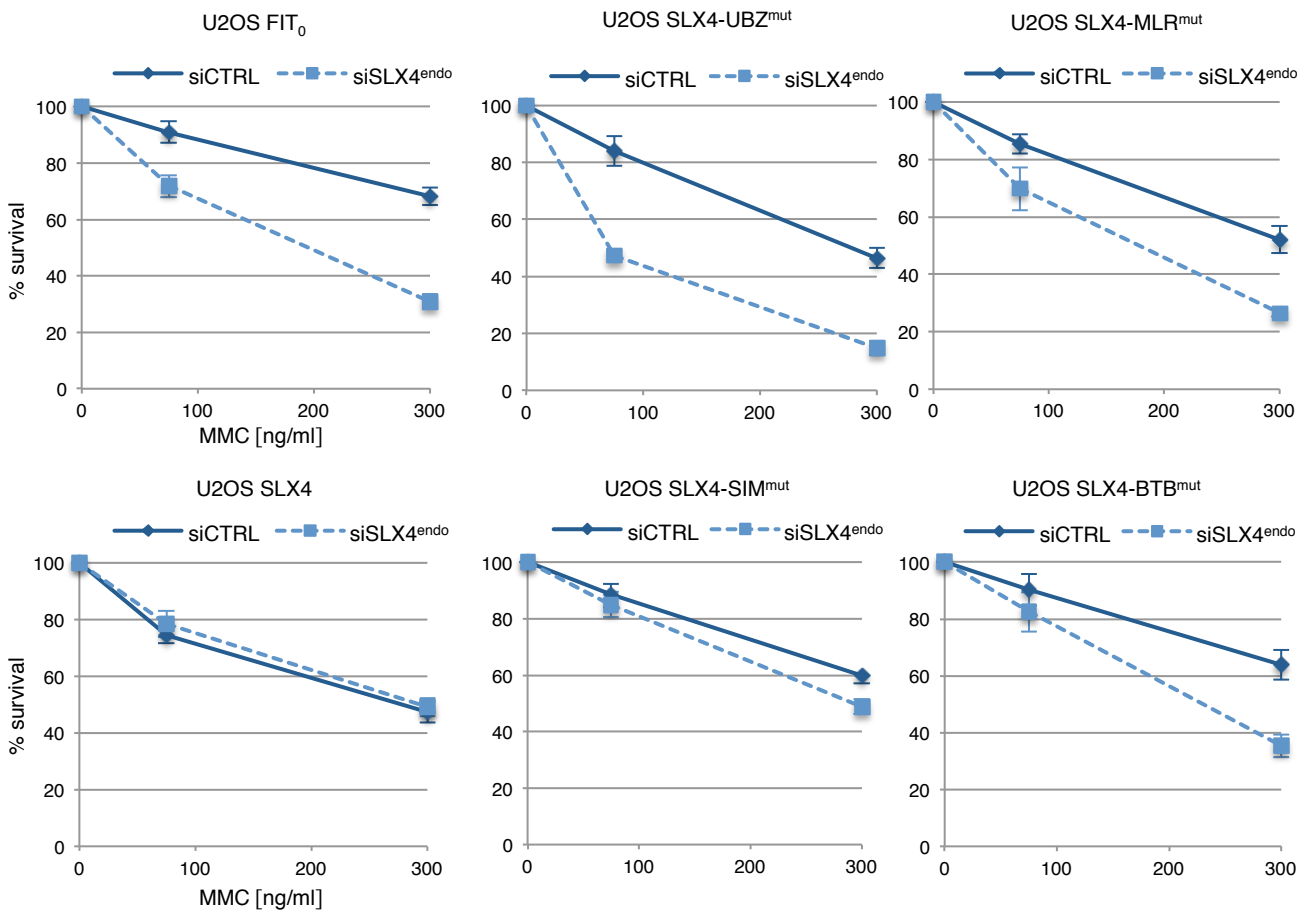


Figure 6

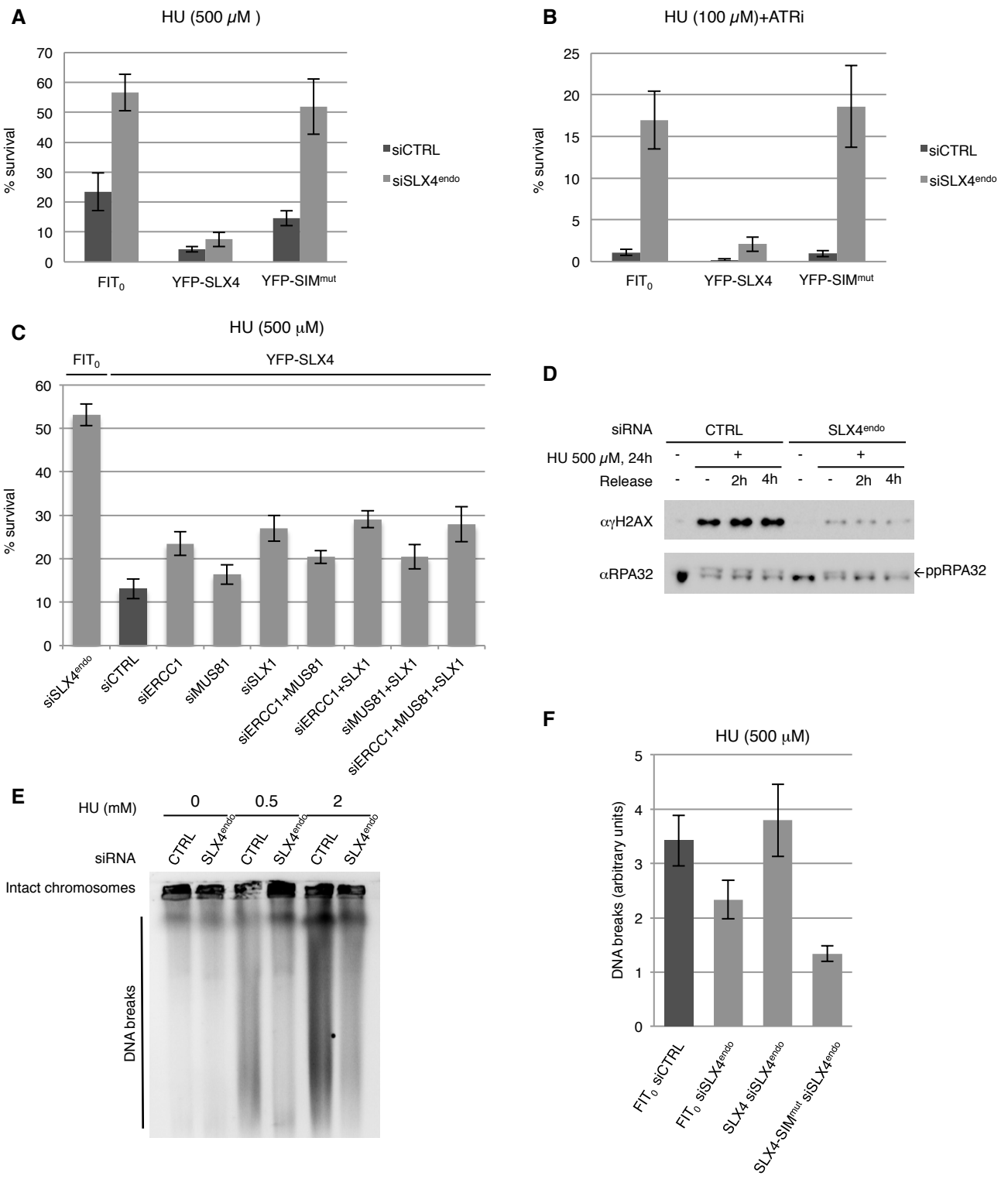
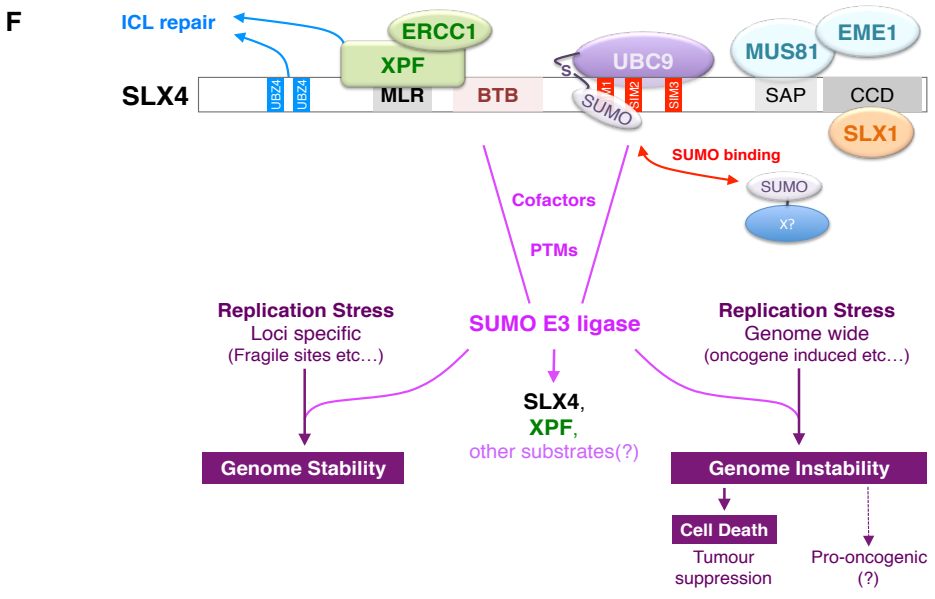
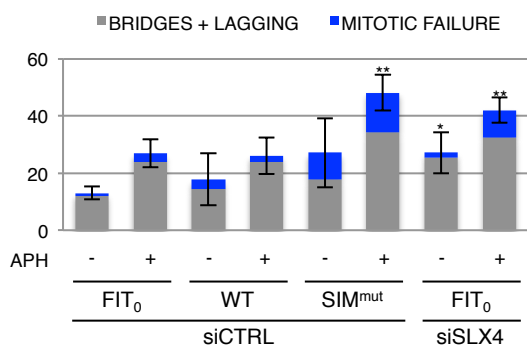
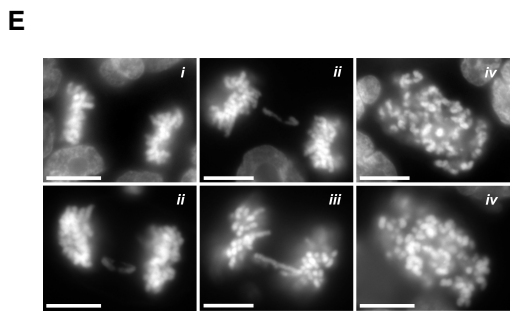
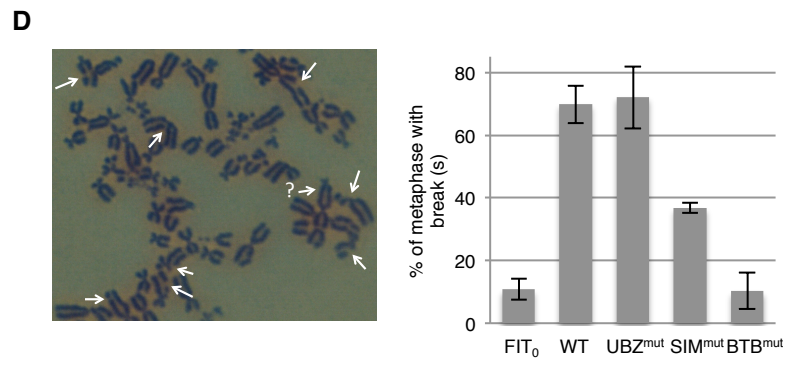
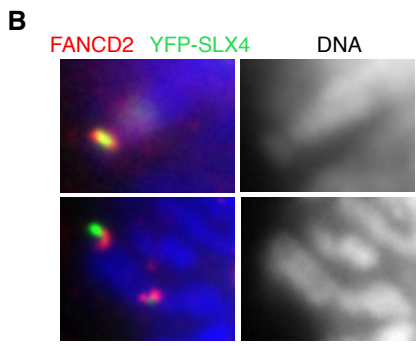
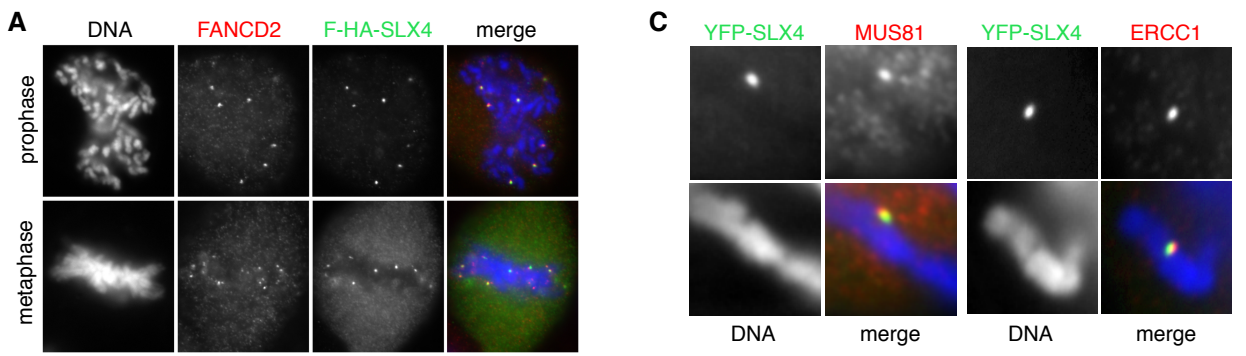
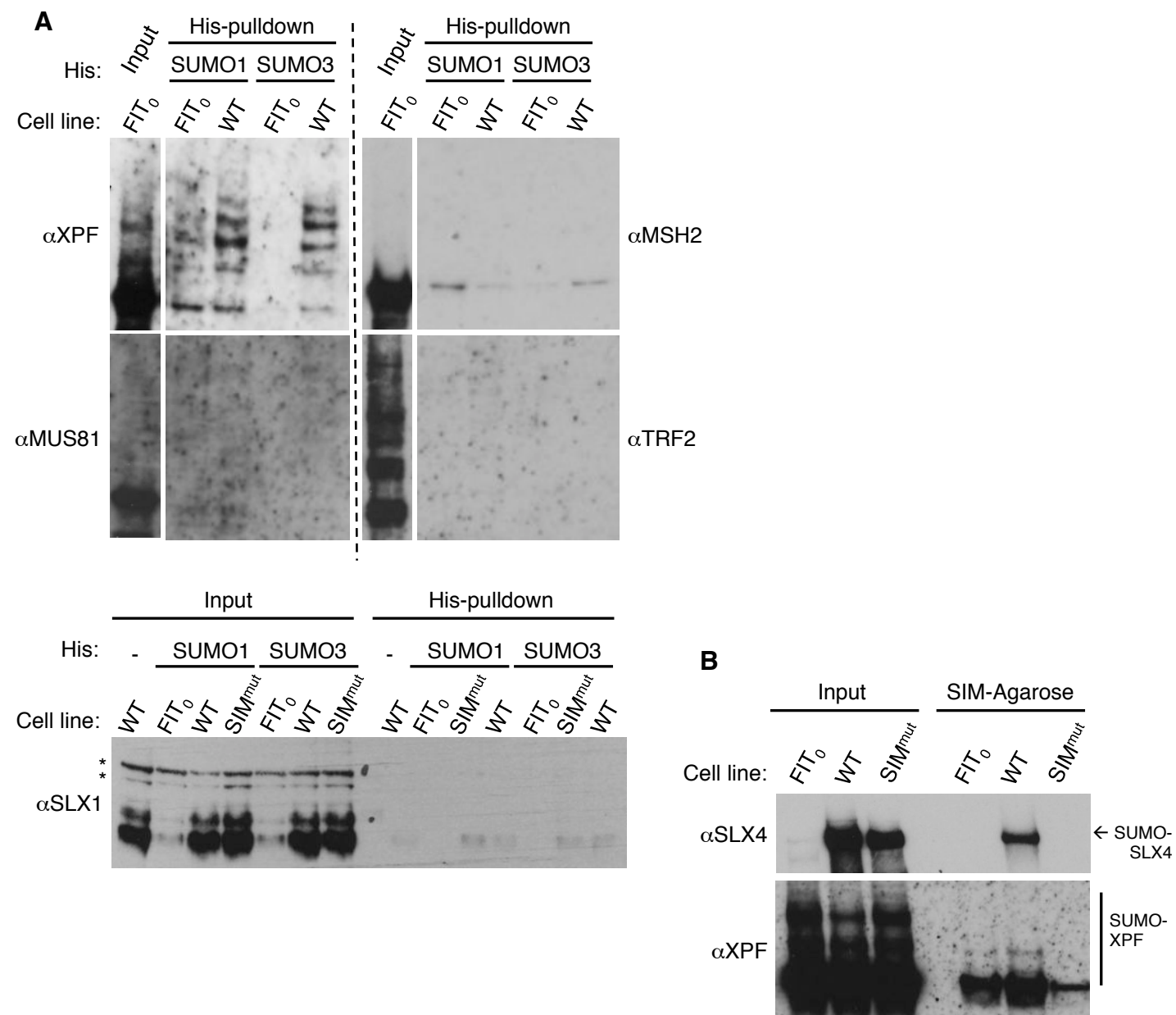


Figure 7



SUPPLEMENTARY INFORMATION

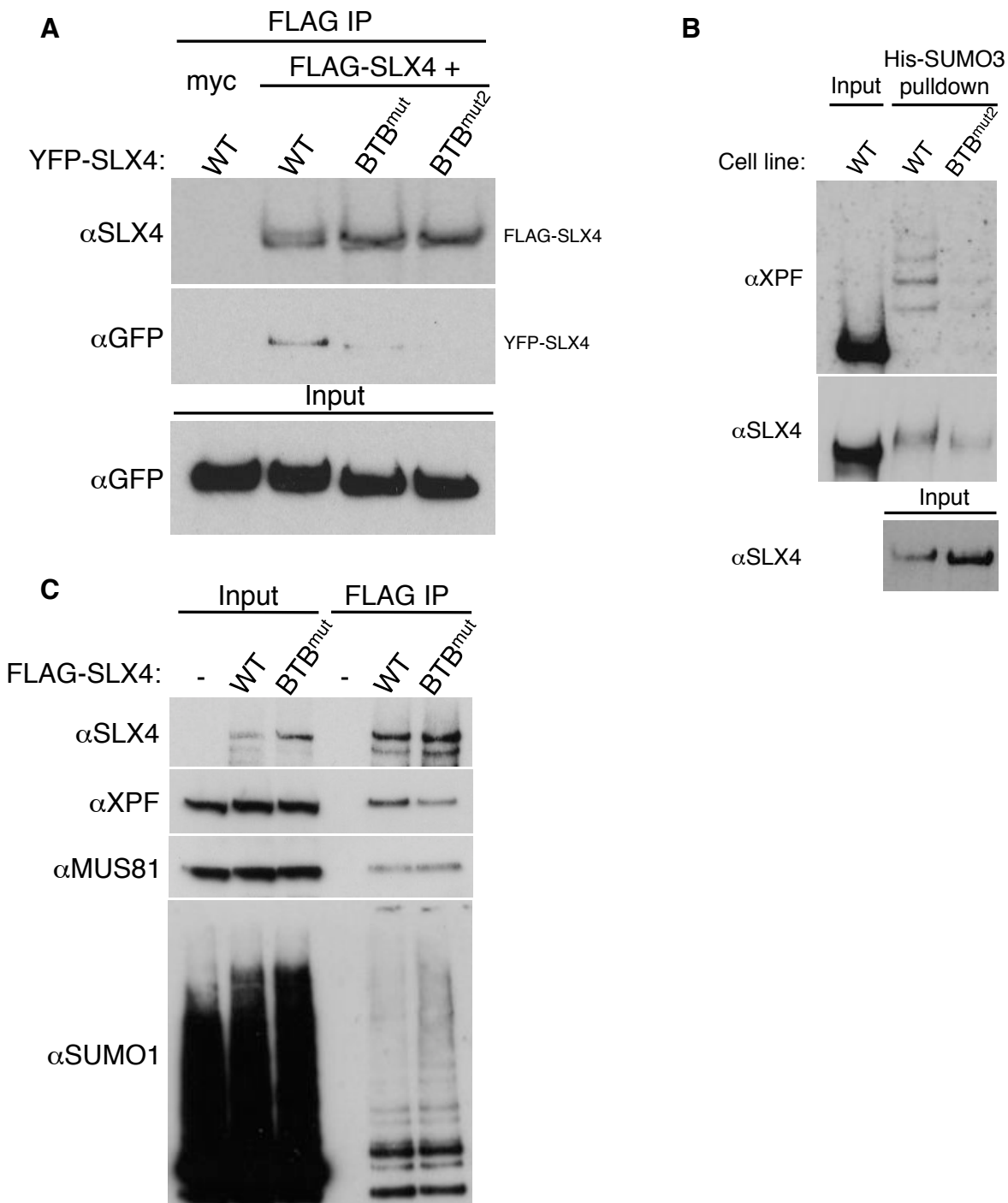
Figure S1 – related to Figure 2



(A) SLX4 overexpression specifically promotes XPF SUMOylation. Upper part: potential SUMOylation of SLX4 direct partners XPF, MUS81, MSH2 and TRF2 was assessed in U2OS *FIT₀* cells and U2OS YFP-SLX4 cells treated with 1 μ g/ml of Dox. Bottom part: YFP-SLX4 overexpression stabilizes endogenous SLX1 but does not promote its SUMOylation. SLX1 SUMOylation was assessed in U2OS *FIT₀*, U2OS YFP-SLX4 and *SIM^{mut}* cells induced with Dox. (*) indicate aspecific bands recognized by anti-SLX1 antibody.

(B) Endogenous SUMOylation of SLX4 and XPF. HeLa cells expressing YFP-SLX4 or *SIM^{mut}* were harvested after 24 h of Dox induction (1 μ g/ml). Nuclei were isolated and lysed in the presence of NEM. Extracts were incubated with SIM peptide agarose beads (Boston Biochem) to purify endogenously SUMOylated proteins. Western blot analysis revealed SUMOylation of SLX4 as well as XPF in cells expressing SLX4 but not in cells expressing a *SIM^{mut}* mutant version of SLX4.

Figure S2 – related to Figure 2

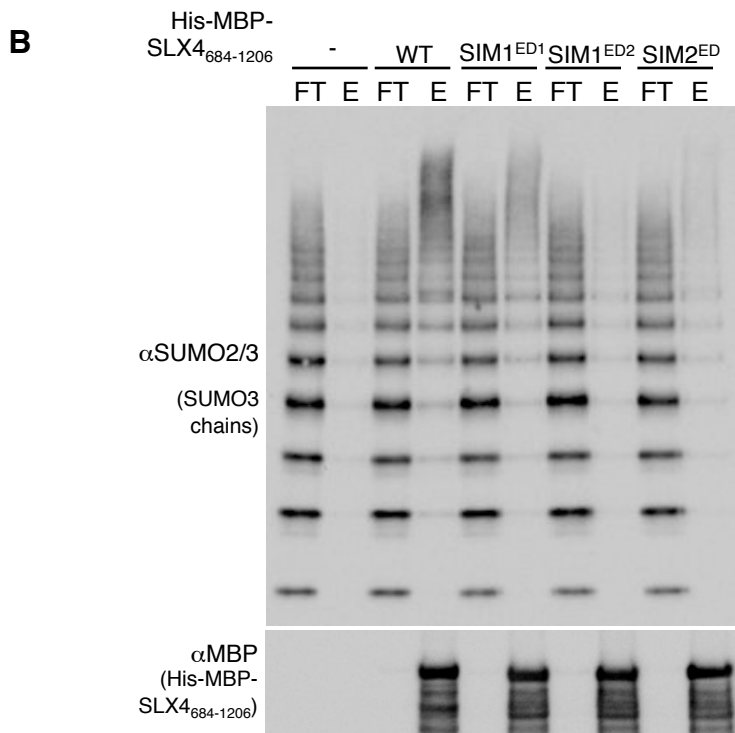
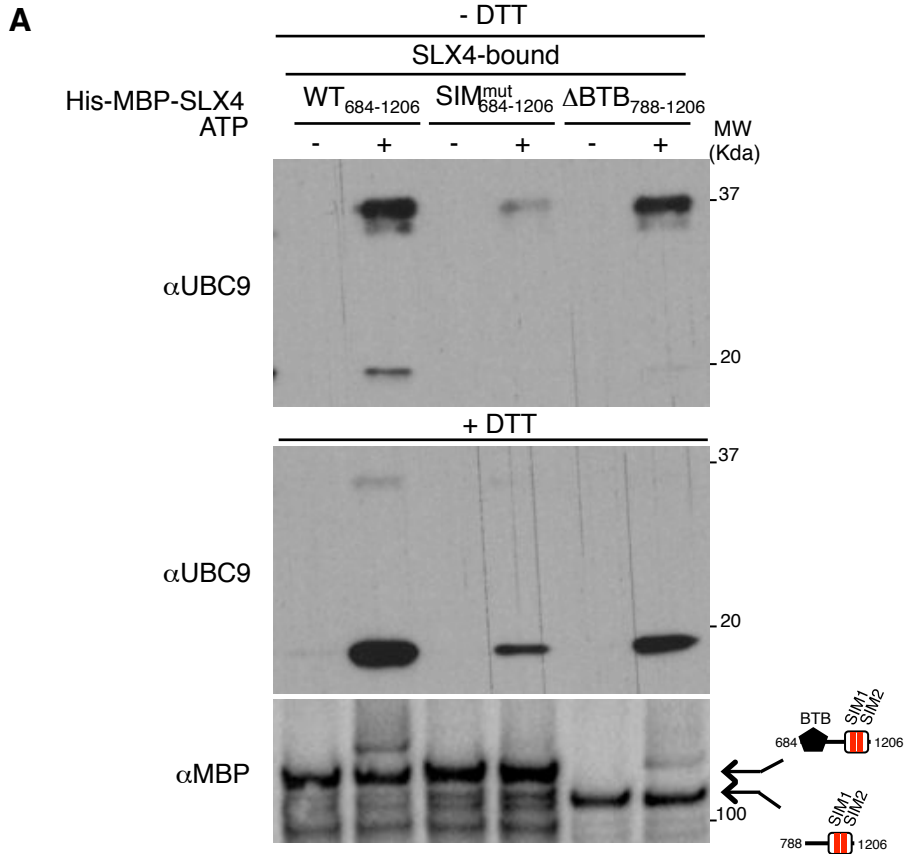


(A) Mutations within the BTB domain impair SLX4 oligomerization. HeLa FIT₀ cells were transiently co-transfected with FLAG-SLX4 and YFP-SLX4, BTB^{mut} or BTB^{mut2} before FLAG-IP and Western blot.

(B) The BTB^{mut2} (YLY→ALA) was poorly SUMOylated and did not promote XPF SUMOylation.

(C) Mutations in the BTB domain of SLX4 does not abolish SUMO binding. FLAG-SLX4 and BTB^{mut} were transiently expressed in 293 cells before FLAG IP and analysis of co-immunoprecipitation of XPF, MUS81 and SUMOylated proteins.

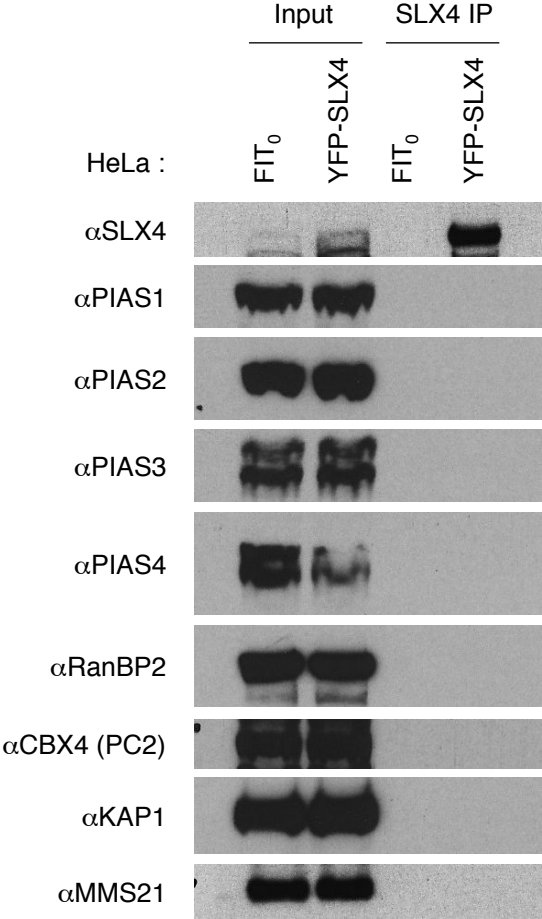
Figure S3 – related to Figure 3



(A) The BTB domain of SLX4 is not required to interact with charged UBC9 (UBC9~SUMO). The experiment was performed as described in Figure 3.

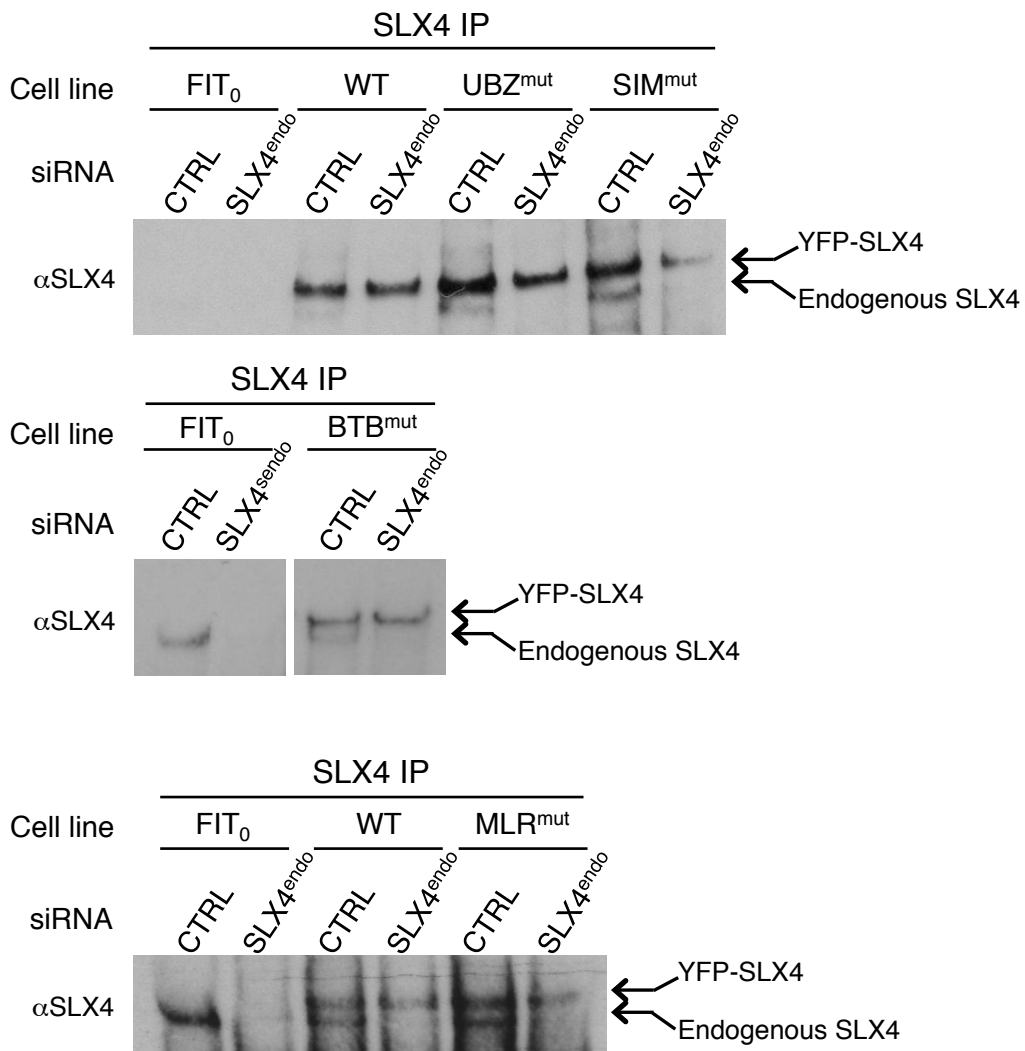
(B) Impact of mutating the acidic residues (E/D) in SIM1 and SIM2 of a His-MBP-SLX4₆₈₄₋₁₂₀₆ fragment on SUMO chain binding. The experiment was performed as described in Figure 1.

Figure S4 – related to Figure 4



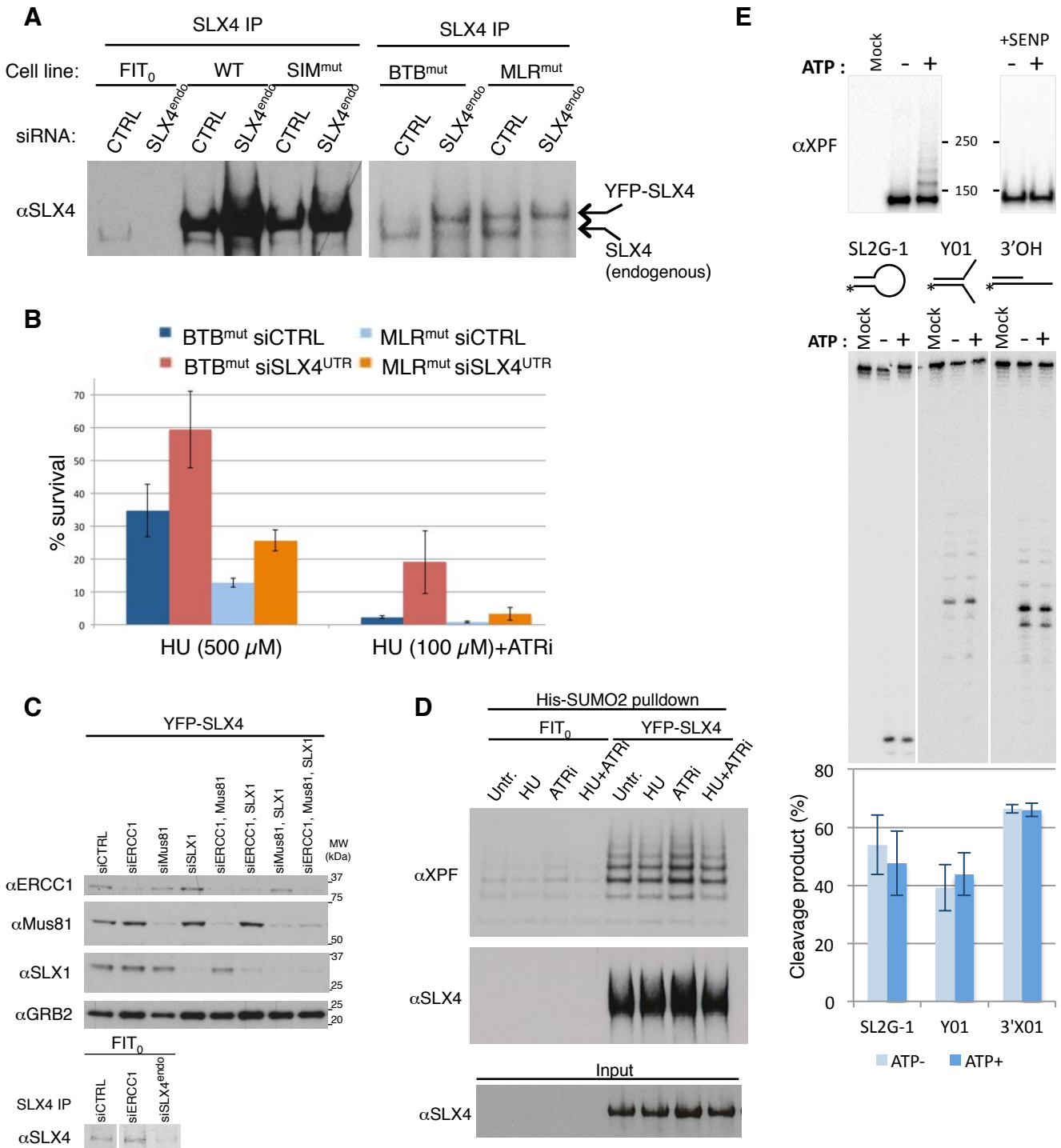
HeLa FIT₀ or YFP-SLX4 cells were induced with doxycycline (1 ng/ml). Lack of co-immunoprecipitation of the indicated SUMO E3 ligases with YFP-SLX4 was checked by western blot.

Figure S5 – related to Figure 5



Examples of endogenous SLX4 depletion with siRNA SLX4^{endo} in MMC survival assays in the indicated U2OS cell lines (refers to Figure 5C).

Figure S6 – related to Figure 6



(A) Examples of endogenous SLX4 depletion in HU survival assays in the indicated HeLa cell lines (refers to Figure 6A and B).

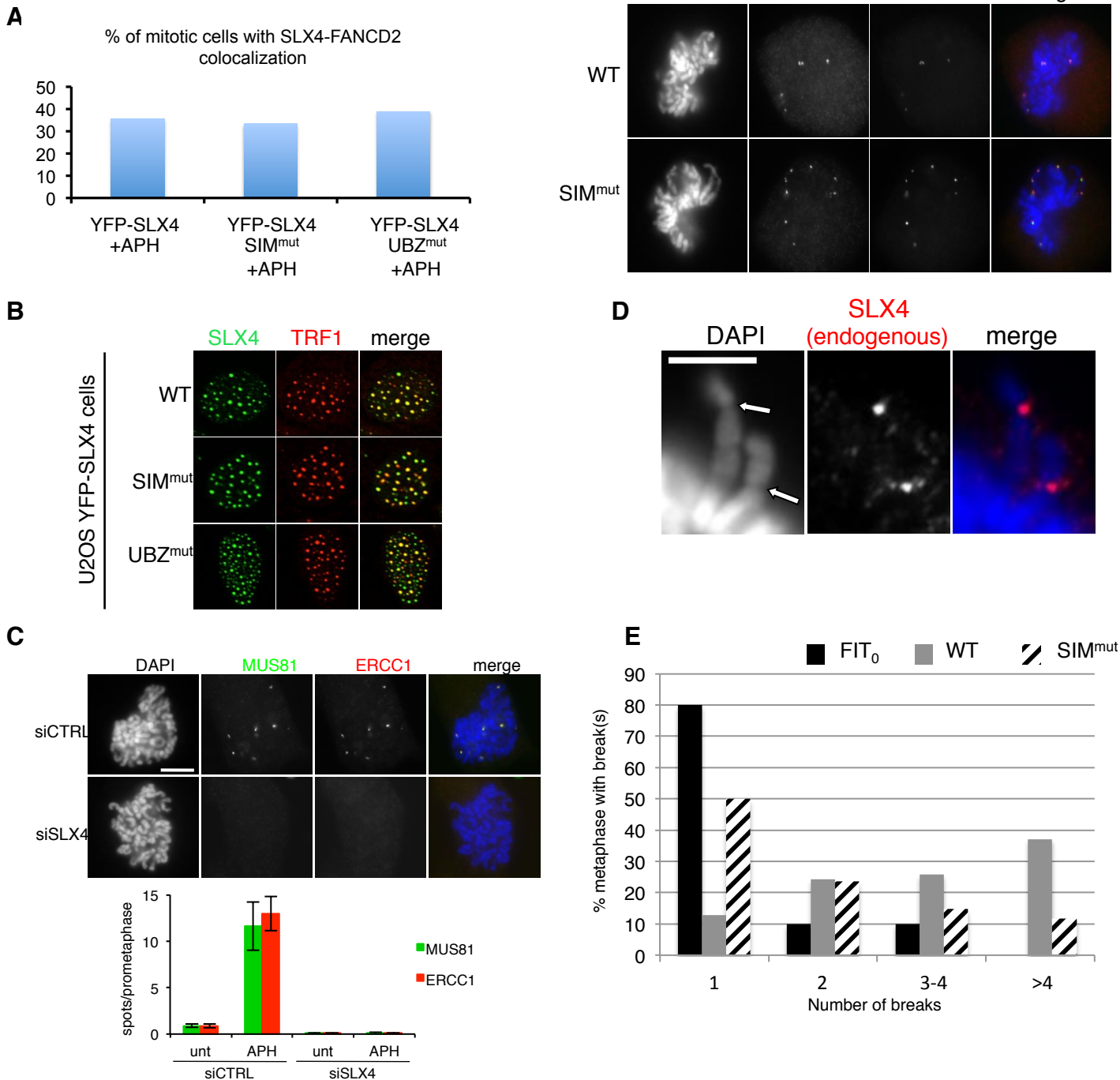
(B) Analysis of HU and HU+ATRi survival in HeLa cells expressing YFP-SLX4 BTB^{mut} or MLR^{mut}.

(C) Depletion controls for colony survival assays in Figure 6C of endogenous SLX4 and its associated endonucleases.

(D) No noticeable modulation of XPF or SLX4 SUMOylation in response to HU, ATRi or HU+ATRi.

(E) Comparison of the nuclease activity of non SUMOylated or SUMOylated XPF-ERCC1. XPF-deficient XP2YO cells were co-transfected with YFP-XPF, Myc-ERCC1 and F-HA-SLX4₁₋₁₄₆₂ (=SLX4 ΔSAPΔCCD unable to interact with MUS81-EME1 or SLX1). YFP-XPF was pulled down with GFP binder, SUMOylated *in vitro* and eluted with Tev protease which cuts between XPF and the YFP tag. SENP (SUMO protease) treatment (upper Western blot) was carried out to collapse SUMOylated XPF into a single band and facilitate the estimation of relative XPF protein levels.

Figure S7 – related to Figure 7



(A) Left: : quantification of YFP-SLX4 and FANCD2 co-localization in APH-treated mitotic HeLa cells. Right: representative images showing the co-localization of YFP-SLX4 and SIM^{mut} with FANCD2 mitotic foci at CFS.

(B) Representative images showing the co-localisation of YFP-SLX4, SLX4-SIM^{mut} and SLX4-UBZ^{mut} with TRF1 in interphasic nuclei.

(C) Upper panel : Representative images showing siCTRL and siSLX4 transfected cells at prometaphase. Cells were treated with 0.3 μ M APH for 24h before fixation and immunostaining for MUS81 and ERCC1. Lower panel : Quantification of MUS81 and ERCC1 spots per prometaphase in untreated and APH-treated cells transfected with siCTRL or siSLX4 siRNAs.

(D) Representative images showing the localisation of endogenous SLX4 at chromatid gaps or constrictions on mitotic chromosomes in APH-treated HeLa cells. DNA (DAPI, blue in the merged image), SLX4 (red in the merged image), and merge are shown from left to right. Scale bar= 5 μ m.

(E) Quantification of the amount of breaks per metaphase found in U2OS FIT₀, U2OS YFP-SLX4 or SIM^{mut} amongst the metaphases presenting at least one break or gap.

SUPPLEMENTARY EXPERIMENTAL PROCEDURES

Cell lines

U2OS, HeLa and 293 Flp-In TRex (FIT₀: parental cells) (kindly provided by Palm Silver, Stephen Taylor and Jean-Pierre Quivy and Geneviève Almouzni respectively) were routinely maintained in DMEM, 10% FBS, Pen/strep (Gibco) + 2 $\mu\text{g}/\text{ml}$ Blasticidin (Invitrogen). To generate stably expressing cells producing YFP or FLAG-HA tagged versions of SLX4, FIT₀ parental cell lines - previously cultured in Zeocin (100 $\mu\text{g}/\text{ml}$ [Invitrogen]) to maintain the genomic FRT site- were co-transfected with plasmid pOG44 (encoding the Flp recombinase) and the pDEST-YFP or F-HA version of SLX4 with a 7:1 ($\mu\text{g}/\mu\text{g}$) ratio, respectively. Selection of recombinant clones was achieved with Hygromycin (200 $\mu\text{g}/\text{ml}$ in U2OS, 100 $\mu\text{g}/\text{ml}$ in HeLa, 100 or 50 $\mu\text{g}/\text{ml}$ in 293 cell lines [Invitrogen]) and pools of selected clones were usually mixed to minimize clonal heterogeneity and obtain a stable population.

Antibodies and western blot

SLX4 (A302-270A, A302-269A) and PC2 (CBX4) (A302-355A) antibodies were purchased from Bethyl, SLX4 antibody recognizing N-terminal domain of SLX4 and SLX1 antibody were kindly provided by John Rouse. Mus81 [MTA30 2G10/3] (ab14387), SUMO1 (ab32058), SUMO2/3 [BA2] (ab81371), MSH2 (ab70270). KAP1 (ab10484), and TRF2 [4A794] (ab13579) antibodies were purchased from Abcam. XPF [clone 219] (XPF Ab-1) antibody was from Thermo scientific. γH2AX [JBW301] (05-636) antibody was from Millipore. MBP (E8038) antibody was from New England Biolabs. p32, subunit of RPA (NA19L) antibody was from Calbiochem. Ubc9 [JBW301] (4786), PIAS1 [D33A7] (3550), PIAS3 [D5F9] (9042) and PIAS4 [D2F12] (4392) antibodies were purchased from Cell signalling technology. His (631212), GFP [JL-8] (632380) antibodies were from Clontech. FLAG (F3165) antibody was from Sigma. GRB2 (610111) antibody was from BD biosciences. ERCC1 [FL-297] (sc-10785) antibody was purchased from Santa Cruz. PIAS2 (NBP2-19819), RanBP2 (NB100-93337) antibody were purchased from Novus biologicals. MMS21 antibody was kindly provided by Patrick Ryan Potts and Hongtao Yu. Goat anti-rabbit IgG/HRP (2019-08) and goat anti-mouse IgG/HRP (2019-05) antibodies were purchased from Dako. Donkey anti-sheep IgG/HRP (sc-2473) antibody was from Santa Cruz. SDS-PAGE and western blotting was done with Novex® NuPAGE® SDS-PAGE Gel System and XCell II™ blot module (Invitrogen), respectively. Hybond-C Extra (RPN203E) was purchased from GE healthcare. Western lightning plus ECL (NEL105001EA) was from PerkinElmer, ECL prime western blotting detection reagent (RPN2232) was from GE healthcare. Hyperfilm ECL (28-9068-35) was purchased from GE healthcare. Chemidoc MP imaging system (Biorad) was also used for detection.

Mutagenesis, cloning and molecular biology

Standard molecular biology techniques were used. A list of primers used in this study is available upon request. Site-directed mutagenesis was first performed to generate SLX4 constructs that are RNAi-resistant to siSLX4-2 used in complementation assays to specifically deplete endogenous SLX4 (siSLX4-2R). For siSLX4-2R, cDNA,

SLX4 natural sequence «TCCAGATCTCAGAAATCTTCATCCAAA » was changed to « TCCAGATCTCAaAAgTcTcTCCAAA », lower cases indicating mutated bases.

The following fragments of SLX4 and silent or point mutations were generated:

_ UBZ^{mut} (C296S, C299S, C336S, C339S)

_ SIM^{mut} (SIM1: V₁₁₅₁ILLL₁₁₅₅ → AAAAA ; SIM2: I₁₁₉₄IDV → AADV ; SIM3: V₁₃₉₂VEV → AAEV)

_ SIM_{1,2,3}^{mut} (SIM1: V₁₁₅₁ILLL₁₁₅₅ → AALLL ; SIM2: I₁₁₉₄IDV → AADV ; SIM3: V₁₃₉₂VEV → AAEV)

_ SIM_{1,2}^{mut} (SIM1: V₁₁₅₁ILLL₁₁₅₅ → AALLL ; SIM2: I₁₁₉₄IDV → AADV)

_ BTB^{mut} (H₇₀₆KFVL₇₁₀ → AAAAA)

_ BTB^{mut2} (Y₇₅₄LY → ALA)

_ « BTB_{lg} » (684-1206)

_ « BTB_{lg} ΔBTB » (788-1206)

_ MLR^{mut} (F₅₂₉LW → ALA)

The following mutations were introduced in pDEST GST-UBC9 plasmid :

C93S (catalytic inactive), K65A and K74A (basic patch mutants)

Protein Expression and Purification

His-MBP-tagged fragments of SLX4 were expressed in *E.coli* (Rosetta) induced with 0.15 mM IPTG at 30°C for 4 h or at 16°C overnight. Bacterial pellets were frozen in PBS. The next day, an equivalent volume of 2x lysis buffer (100 mM Tris [pH=8], 20% [v/v] glycerol, 2% [v/v] Triton X-100, 1 M NaCl, 1 mg/ml lysozyme (Sigma)) was added. Lysates were sonicated and clarified. Supernatants were incubated with an amylose resin (Clontech) and washed 5 times in wash buffer (50 mM Tris [pH=8], 1 M NaCl, 0.01% [v/v] Triton X-100). Elution was performed with 20 mM maltose in elution buffer (50 mM Tris [pH=8.0], 0.01% [v/v] Triton X-100). A second round of purification was performed with Cobalt columns (TALON, Clontech) before elution with 100 mM Imidazole. Purified SLX4 fragments were aliquoted, flash-frozen in liquid nitrogen and stored at -80°C.

For UBC9 purification, GST-UBC9 was purified on Glutathione agarose (Molecular probes) before cleavage with the TEV protease to get rid of the GST tag.

In vitro interactions with SUMO chains

Purified SLX4 fragments (4.5 μg) were incubated in SUMO binding buffer (50 mM Tris HCl [pH=7.4], 250 mM NaCl, 0.1% [v/v] NP-40, 2 mM DTT, 5% [v/v] glycerol) {Tatham:2008gg} with 250 ng of SUMO-2 or SUMO-3 chains (Boston Biochem). Incubations were performed at 4°C for 105 min in a final volume of 225 μL. Purified SLX4 fragments were captured on an amylose resin (Clontech). Amylose beads were washed 6 times in SUMO binding buffer before elution in sample buffer (Invitrogen).

Ex vivo/in vitro SUMOylation assay

YFP epitope-tagged SLX4 complexes were purified from either HeLa FIT₀ cells transiently expressing pDEST-YFP-SLX4 or HeLa cell lines stably expressing YFP-SLX4 with doxycycline-inducible manner (1 ng/ml of doxycycline [Sigma]). For immunoprecipitation, cells were washed with PBS and lysed with NETN buffer (50 mM Tris-HCl [pH 8.0], 150 mM NaCl, 1 mM EDTA, 1% NP-40, 1 mM DTT, 0.25 mM PMSF) containing a proteasome inhibitor cocktail (Roche). After centrifugation,

supernatants were incubated with GFP binder (kindly provided by Mauro Modesti) for 2 h at 4°C. The beads were washed 3 times with NETN buffer, twice with TBS and 5 times with 50 mM Tris-HCl [pH 8.0], then SLX4 complexes immobilized on the beads were incubated for the indicated times at 37°C in a standard reaction mixture containing 50 mM Tris-HCl [pH 7.6], 10 mM MgCl₂, 0.2 mM CaCl₂, 4 mM ATP, 1 mM DTT, 228 nM of E1 (SAE1/UBA2: Boston Biochem), 2.5 μM of E2 (Ubc9: Boston Biochem), and 12.5 μM of SUMO2 (Boston Biochem). In Figures 4E, 4F and 4G, NETN buffer including 850 mM NaCl was added to the supernatant before immunoprecipitation to adjust the final concentration of NaCl to 500 mM. After the incubation, beads were washed with NETN including 500 mM NaCl, TBS and 50 mM Tris-HCl [pH 8.0], then *in vitro* SUMOylation assay was carried out as described above. In Figure 4F and 4G, digested or undigested plasmid DNA (pcDNA6.2/EmGFPDest [Invitrogen]) at a final concentration of 95 ng/μL was preincubated with immunoprecipitated YFP-SLX4 complex just before *in vitro* SUMOylation reaction within the buffer containing 50 mM Tris-HCl [pH 7.6], 10 mM MgCl₂, 0.2 mM CaCl₂, 1 mM DTT (buffer A). In Figure 4H, lambda phosphatase (λPP; NEB) or heat-inactivated λPP was incubated with YFP-SLX4 complex in buffer A containing 1 mM MnCl₂ before 50 mM Tris-HCl [pH 8.0] wash.

Two-steps SUMOylation assays and UBC9 *in vitro* binding

To investigate a putative interaction between SLX4 and UBC9~SUMO, two-steps reactions were preformed (Figure 4C). First, *in vitro* SUMOylation assays were carried out in a reaction mixture containing 20 mM Hepes pH=7.6, 5 mM MgCl₂, 225 nM E1, 1.5 μM UBC9, 12.5 μM SUMO2, 5 mM ATP for 1 h at 32°C. Meanwhile, 28 pmol of His-MBP-tagged SLX4⁶⁸⁴⁻¹²⁰⁶ was immobilized on amylose beads saturated with BSA. Amylose beads was then washed and resuspended in 100 μL of binding buffer (20 mM Tris [pH=7.5], 50 mM NaCl, 4 mM MgCl₂, 0.5% NP-40 and 1 mg/ml BSA). 9 μl of the SUMOylation mix (E1, E2, SUMO2, +/- ATP) was then added to the reaction (SLX4-UBC9~SUMO binding mixture) and further incubated for 1 h at RT. Amylose beads were washed 3 times with binding buffer before elution in sample buffer. Flow-through fractions were also kept to analyze the SLX4-unbound material.

Transient transfections and co-immunoprecipitation

293 cells were transfected with JetPEI (Polyplus transfection) or lipofectamine 2000 (Invitrogen). Cells were lysed 24 h to 48 h post transfection in NETN buffer (50 mM Tris-HCl [pH=8.0], 150 mM NaCl, 1 mM EDTA, 0.5% [v/v] NP-40) before sonication and clarification by centrifugation. Immunoprecipitations (IPs) were performed with anti-FLAG M2 beads (Sigma), GFP binder (kindly provided by Mauro Modesti) or anti-SLX4 (Bethyl, A302-269A) for a few hours or overnight at 4°C. Beads were extensively washed with NETN buffer before elution in loading buffer or elution with a 3xFLAG peptide (Sigma) in the case of Flag IPs.

To look at the co-IP of SUMOylated proteins and UBC9, lysate was prepared with NETN buffer supplemented with 30 mM N-Ethylmaleimide (NEM, from Sigma).

***In vivo* SUMOylation**

U2OS or HeLa cells were seeded in 60 mm or 100 mm dishes. A day later, cells were transfected with His-SUMO1+UBC9 or His-SUMO3+UBC9. UBC9 was co-transfected to increase the level of global SUMOylation thereby facilitating the detection of

SUMOylated proteins. At the time of transfection, doxycycline was added at 1 $\mu\text{g/ml}$ to achieve robust exogenous SLX4 overexpression. Cells were collected 24 h later and cell pellets were either frozen at -80°C for subsequent analysis or directly lysed in denaturing Urea buffer (8 M Urea, 115 mM NaH_2PO_4 , 300 mM NaCl, 10 mM Tris-HCl [pH=8.0], 0,1% [v/v] NP-40, 5 mM Imidazole) for 1 h at RT. Extracts were briefly sonicated before centrifugation. Cleared extracts were incubated with TALON metal affinity resin (Clontech) for 35 min at RT. Beads were washed 3 to 4 times with denaturing Urea buffer before elution in loading buffer supplemented with 30 mM EDTA.

siRNA transfections

The following siRNA sequences were used in this work: siCTRL (Negative control Med GC; Invitrogen 12935-300) and siSLX4-2 (CAGATCTCAGAAATCTTCATCCAAA) are Stealth siRNA synthesized from Invitrogen. Also, siRNAs targeting the 5'UTR and 3'UTR of SLX4 were used:

SLX4 UTR87 (GCACCAGGUUCAUAUGUAUdTdT) and SLX4 UTR7062 (GCACAAGGGCCAGAACAAdTdT), with siLUC (CGUACGCGGAAUACUUCGAdTdT) as a negative control.

For ERCC1 and MUS81 knockdown, cells were simultaneously transfected with siERCC1 (siGENOME Human ERCC1 M-006311-00) and siMus81 (siGENOME SMA M-016143-01) (smartpool from Dharmacon), respectively.

SLX1-targeting siRNAs were used:

si1#1: GGCGTCTACCTGCTCTACTGCCTGA,
si1#2: TCAACACTGCTCGTCCGGTCCAGCA,
si1#3 : GCACACTGGACAGACCTGCTGGAGA.

siRNAs were transfected at a concentration of 5 nM (siSLX4-2), 20 nM (siUTRs) or total 30 nM (Figure 6C) using INTERFERin (Polyplus transfection) according to manufacturer's instructions.

Cell survival, clonogenic assay

For the doxycycline dose-response experiments (Figures 5A and B), cells were seeded at low density (600 to 800 cells per 60 mm Petri dish) in the presence or absence of doxycycline.

For the mitomycin C (MMC) complementation assay (Figure 5C), U2OS cells were transfected with non-targeting stealth siRNA versus stealth siSLX4-2 at 5 nM. Two days later, cells were trypsinized and reseeded at 600 cells per 60 mm Petri dishes with 2 ng/ml of doxycycline. One day later, cells were treated with 75 or 300 ng/ml MMC (Sigma) for 1 h. Cells were subsequently washed with PBS and cultured with fresh medium including 1 ng/ml of doxycycline. Colonies were fixed and counted 7 to 10 days later.

For experiments performed in HeLa cells (Figures 6A and 6B), a combination of siRNAs SLX4 UTR87 and UTR7062 (siSLX4^{UTRs}) were used versus siLUC. Cells were transfected twice with CTRL (siLUC) or SLX4^{UTRs} siRNAs (20 nM) and then seeded at low density in medium containing 1 ng/ml doxycycline. The day later, cells were treated for 24 h with the indicated dose of hydroxyurea (HU [Sigma]) eventually combined with the ATR inhibitor VE-821 (Selleckchem). Cells were then washed and allowed to grow before staining of the colonies 7 to 10 days later. From the seeding in Petri dish, doxycycline is maintained at 1 ng/ml during the experiments.

Because even low doses of doxycycline (low SLX4 overexpression) induce a noticeable toxicity in HeLa cells, HeLa cells expressing YFP-SLX4 or MLR^{mut} were seeded at 1200 cells per Petri while HeLa FIT₀, YFP-SLX4 SIM^{mut} and YFP-SLX4 BTB^{mut} were seeded at 800 cells per Petri to normalize colony number in untreated conditions.

In Figure 6C, HeLa FIT₀ cells were seeded and siRNA transfection (total 30 nM) were carried out twice at 24 and 48 h after seeding (siLUC was used as a negative control and siSLX4^{UTRs} for SLX4 depletion). 6 h after 2nd siRNA transfection, cells were reseeded at 800 cells for FIT₀ cells or at 1200 cells for cells expressing YFP-SLX4 per 60 mm Petri dish. 18 h later, doxycycline induction and HU treatment were carried out as described in Figure 6A and 6B.

All experiments were performed in duplicates or triplicates and independent experiment were achieved 3 to 8 times.

Metaphase spreads and chromosome breakage

Cells were seeded in medium containing 10 ng/ml doxycycline for 48 h. Colcemide (Gibco) was added at 0.1 μ g/ml for 3 h before collecting the cells, PBS washing and resuspension in 75 mM KCl for 15 min at 37°C. Cells were then fixed with fresh Methanol/Acetic Acid (v/v=3:1) and frozen at -20°C for at least 16 h. Pellet was then further washed with fresh fixative before dropping onto slides. Chromosomes were stained with 5% Giemsa (Gibco) before extensive wash and mounting. Obvious gaps and breaks were scored.

Pulse field gel electrophoresis

FIT₀ cells and cells stably expressing YFP-SLX4 or SIM^{mut} with doxycycline-inducible manner (1 ng/ml of dox) were transfected with either siLUC or siSLX4^{UTRs}. 48 h after siRNA transfection, cells were reseeded at low cell density and treated with or without HU (500 μ M) for 24 h. After the treatment, cells were trypsinized, washed with PBS including 50 mM EDTA [pH 8.0], and resuspended in 50 μ l of cell suspension buffer (10 mM Tris-HCl [pH 7.2], 20 mM NaCl, 50 mM EDTA) and equal volume of low-melting-point agarose (1% final concentration) (Sigma) at a concentration of 1 x 10⁶ cells per plug. Plugs are treated with Proteinase K (1 mg/ml) in PK buffer (100 mM EDTA [pH 8.0], 0.2% sodium deoxycholate, 1% N-Lauroylsarcosine sodium salt [Sigma]) for 24 to 48 h at 50°C and washed 4 times with wash buffer (20 mM Tris-HCl [pH8.0], 50 mM EDTA), then loaded onto 1% agarose gel. PFGE was performed on a BioRad CHEF DR-III system in 0.5 x TBE (Euromedex) at 14°C using the following program: 20 h at 4 V/cm, 120° angle, 60 to 240 seconds switch time. The separation of broken DNA from intact genomic DNA was visualized by ethidium bromide staining.

Nuclease assay

SUMOylated or unSUMOylated XPF complexes were prepared from SV40-immortalized XP-F (XP2YO) fibroblasts transiently expressing FLAG-HA-SLX4₁₋₁₄₆₂, YFP-XPF and Myc-ERCC1 as described above with the following modifications. Briefly, cells were lysed with NETN buffer and the lysate was incubated with GFP binder for 2 h at 4°C. After washing with NETN and TBS, YFP-XPF complexes retained on the GFP binder resin were subjected to *in vitro* SUMOylation reaction with or without ATP for 40 h at 4°C. The beads were washed 5 times with wash buffer

(20 mM Tris-HCl [pH 8.0], 150 mM KCl, 2 mM MgCl₂, 10% glycerol, 0.1 mM PMSF, 0.5 mM DTT, 0.01% Triton X-100, protease inhibitor cocktail [Roche]) then YFP-XPF complexes were eluted by cleavage with Tev protease. For nuclease assay, ³²P-labelled DNA substrates (SL2G-1, Y0-1 and 3'OH) were prepared as described previously (Coulon et al., 2002). YFP-XPF complexes were incubated with the DNA substrates for 45 minutes at 30°C in a standard reaction mixture containing 50 mM Tris-HCl [pH 8.0], 100 µg/ml BSA, 1 mM β-mercaptoethanol and 0.5 mM MgCl₂. DNA fragments were separated on a denaturing 12% polyacrylamide gel, and the dried gels were analyzed with Phosphorimager (BIORAD). To facilitate the comparison of the amount of SUMOylated or unSUMOylated XPF, the samples were incubated with SENP1 (sentrin/SUMO-specific protease1) Catalytic Domain (6His-SENP1CD from R&D Systems) in a cleavage reaction mixture containing 50 mM Tris-HCl [pH 8.0], 100 mM NaCl, 1 mM DTT, 3 mM MgCl₂ for 15 min at 37°C, to collapse SUMOylated XPF into a single band of unmodified XPF.

Immunofluorescence

Immunofluorescence experiments were performed on cells grown on glass coverslips as described previously (Naim and Rosselli, 2009). For immunostaining, the following primary antibodies were used: rabbit anti-FANCD2 (1:1000, ab2187, Abcam), rabbit anti-ERCC1 (1:100, sc-10785, Santa Cruz), mouse anti-ERCC1 (1:100, sc-17809, Santa Cruz), mouse anti-MUS81 (1:100, ab14387, Abcam), and rabbit anti-BTBD12 (1:500, NBP1-28680, Novus Biologicals). All incubations were performed overnight at 4°C with antibodies diluted in PBS containing 3% BSA and 0.05% Tween-20. Alexa 488- or 594-conjugated anti-mouse and anti-rabbit secondary antibodies were purchased from Molecular Probes. Images were captured using a Zeiss Axio Imager Z1 microscope with a 63x/1.4 NA oil immersion objective equipped with a Hamamatsu camera. Acquisition was performed using AxioVision (4.7.2.). Images were imported into Photoshop (Adobe Systems), processed and merged using the same software.

For gene knockdown in immunofluorescence experiments (Figure 7), the following siRNAs were used: control siRNA (siLacZ 5'-CGUCGACGGAAUACUUCGA-3', Eurogentec); ON-TARGETplus Human SLX4 (84464) siRNA SMARTpool (L-014895, 5'-UCAGAGCCGUCCCAAUAA-3', 5'-CAAGUGAGCCCGAGGAACA-3', 5'-GCGGAGACUUUGUUGAAAU-3', 5'-UCAACGGCACUCAGAUAA-3', Dharmacon). siRNA transfection was performed using Interferin (Polyplus) according to manufacturer's instructions.

For Aphidicolin (APH) treatment, cells were exposed to 0.3 µM APH for 24 h.

To examine the telomeric localization of SLX4, SLX4 SIM^{mut} or UBZ^{mut}, U2OS YFP-SLX4 cells were fixed in methanol before immunofluorescence performed with anti-TRF1 antibody (1:300, ab10579, Abcam)